THESIS FOR THE DEGREE OF DOCTOR OF PHILOSOPHY (PHD)

Examination of transglutaminases in proliferative vitreoretinopathy and neutrophil extracellular trap formation

by Bernadett Márkus

Supervisor: Éva Csősz, PhD

UNIVERSITY OF DEBRECEN
DOCTORAL SCHOOL OF MOLECULAR CELL AND IMMUNE BIOLOGY

DEBRECEN, 2017

Contents

Abbreviations

2-DE: Two-dimension gel electrophoresis

$BPNH_2$: 5-(biotinamido)pentylamine

Ctrl: Control

CTSG: Cathepsin G

Cys: Cysteine

DTT: Dithiothreitol

ECM: Extracellular matrix

ELANE: Neutrophil elastase

ESI: Electrospray ionization

FA: Formic acid

Gln: Glutamine

GO: Gene ontology

IAA: Iodoacetamide

IEF: Isoelectric focusing

Lys: Lysine

LYS: Lysozyme

m/z: Mass-to-charge

MALDI: Matrix-assisted laser desorption/ionization

Met: Methionine

MMPs: Matrix metalloproteases

MPO: Myeloperoxidase

MS: Mass spectrometry

MW: Molecular weight

NETs: Neutrophil extracellular traps

OCT: Optical Coherence Tomography

PMA: Phorbol-12-myristate-13-acetate

Psi: Pound per square inch

PTMs: post-translational modifications

PUT: Putrescine

PVR: Proliferative vitreoretinopathy

RT: Room temperature

SPD: Spermidine

SPM: Spermine

TG1: Transglutaminase 1

TG2KO: TG2 knock-out

TG2: Transglutaminase 2

TGases: Transglutaminases

WT: Wild-type

1. Introduction

The Ca^{2+}-dependent transglutaminases (TGases) are multifunctional enzymes having role in physiological and pathological processes. TGases can catalyze the crosslinking of proteins leading to isopeptide bond formation. They can exert their effect via interaction with substrates and interaction partners as well.

TGases can contribute to numerous human diseases especially autoimmune-, inflammatory-, chronic degenerative-, malignant- and metabolic diseases. The proliferative vitreoretinopathy (PVR) is an abnormal wound-healing response in eye which can occur as a serious complication after surgery for retinal detachment. The exact pathogenesis of PVR is still not completely clarified. TG2 is known to be located in human PVR membranes where takes part in tissue stabilization and would healing processes, but its exact role has not been understood yet.

Neutrophils are one of the first responders in immune response against pathogens. They are activated upon inflammatory stimuli leading to formation of neutrophil extracellular traps (NETs) which is a unique form of cell death. During this process, neutrophils can eject the mixture of nucleoplasm and cytoplasm components resulting in a web-like structure which can trap, neutralize and eliminate the invading pathogens.

Proteomic-based approaches including the classical two dimensional gel electrophoresis (2-DE) and mass spectrometry (MS) can help to understand the physiological and pathological processes leading to the identification and characterization of proteins. During my work I focused on the investigation of the role of TGases in proliferative vitreoretinopathy and neutrophil extracellular trap formation.

2. Theoretical background

2.1 Transglutaminases

Transglutaminases (TGases) are a family of enzymes that can catalyze the posttranslational modification of proteins via the formation of ε-(γ-glutamyl)-lysine isopeptide cross-links between lysine (Lys) and glutamine (Gln) residues in Ca^{2+}-dependent reaction [1]. This bond as well as cross-linked protein products are highly resistant to chemical and physical degradation [2]. All members of the TGase superfamily have a structural homology with the papain-like cysteine (Cys) proteases that is based on catalytic triads (Cys-histidine-aspartic acid or Cys-histidine-asparagine) for acyl-transfer reaction [3]. They have also a conserved tryptophan which is essential for this catalytic reaction [4].

Transglutaminases have been identified in microorganisms [5], plants [6], invertebrates [7] and vertebrates [8]. Nine different TGase isoenzymes have been characterized [3,9]: TGase Factor XIIIa (plasma TGase) that can stabilize fibrin clots and participate in wound healing, the keratinocyte TGase (TG1) involved in the terminal differentiation of keratinocytes and the ubiquitous tissue TGase (TG2) with various functions such as cell differentiation, extracellular matrix stabilization, adhesion, apoptosis and signaling. The epidermal hair follicle TGase (TG3) participates in the terminal differentiation of the keratinocytes and formation of cornified envelope, the prostatic secretory TGase (TG4) plays a role in fertility. TGase 5 plays a role in keratinocyte differentiation and the formation of cell envelope, TGase 6 is expressed in the central nervous system and the recently discovered TGase 7 has role in metal ion binding and the conjugation of polyamines to proteins. Finally, there is a TGase-like protein, the erythrocyte protein band 4.2 that has no enzymatic activity and is an inactive form of TGase due to the presence of alanine instead of Cys in the active site (Table 1).

Gene name	Protein name	Alternative names	Prevalent function	Tissue distribution	Pathology
F13A1	FXIIIa	Factor XIIIa, plasma transglutaminase	Blood clotting and wound healing [10]	Astrocytes, chondrocytesmacrophages, osteoblasts, osteoclasts, synovial fluid, placenta and platelets [11]	Impaired wound healing [12], intramuscular haematomas and subcutaneous [13], severe bleeding tendency [14] and spontaneous abortion [15]
TGM1	TG1	Keratinocyte transglutaminase, transglutaminase type 1, TG1	Cell envelope formation, differentiation of keratinocytes [10]	Membrane-bound keratinocytes [11]	Lamellar ichthyosis [16]
TGM2	TG2	Tissue transglutaminase, transglutaminase type 2, TG2	Cell differentiation, extracellular matrix stabilization and remodeling, adhesion, apoptosis and signaling [17]	Cytosolic, extracellular, membrane and nuclear [18]	Autoimmune diseases, malignancies, metabolic- and neurodegenerative diseases [19]
TGM3	TG3	Epidermal transglutaminase, transglutaminase type 3, TG3	Cell envelope formation, differentiation of keratinocytes [20]	Brain, epidermis, hair follicle [20]	Dermatitis herpetiformis [21]
TGM4	TG4	Prostate transglutaminase, transglutaminase type 4, dorsal prostate protein 1, TG4	Reproduction and semen coagulation [22]	Prostate [22]	Prostate cancer [23]
TGM5	TG5	Transglutaminase type 5, TG5	Keratinocyte differentiation and the cornified cell envelope assembly [20]	Foreskin keratinocytes, epithelial barrier lining [20]	Darier's disease lesions, ichthyosis and psoriasis, [24]
TGM6	TG6	Transglutaminase type 6, TG6	Central nervous system development and motor function [25]	Testis and lung [26]	Polyglutamine (polyQ) diseases [27] and spinocerebellar ataxias [28]
TGM7	TG7	Transglutaminase type 7, TG7	Not characterized	Testis and lung [26]	Breast cancer [29]
EPB42	Band 4.2	B4.2, ATP-binding erythrocyte membrane protein band 4.2	Cell attachment, membrane integrity and signal transduction [10]	Bone marrow, erythrocyte membranes, foetal liver, membrane and spleen [11]	Spherocytic elliptocytosis [30]

Table 1. Transglutaminase isoenzymes, their function, physio-pathological relevance and tissue distribution.

2.2 Substrates and interaction partners of transglutaminases

The substrates and interaction partners of transglutaminases have been identified in intracellular compartments such as cytosol, nucleus and mitochondria, on the cell surface and in the extracellular matrix as well [31]. For the detection of the functional role of TGases in different types of cells and tissues, identification of their substrates and interactors is important. In addition, recognition of these proteins would give us a better understanding on the role of TGases in numerous pathological states leading possibly to the determination of novel drug targets and diagnostic markers.

TRANSDAB database (http://genomics.dote.hu/wiki) has been generated to collect information about TGase substrate proteins and interaction partners. It contains more than 500 articles about 340 substrates and almost 80 interactors for TGases FXIIIa, TG1, TG2, TG3, TG4, TG5 and microbial TGase [32].

2.3 The function of transglutaminases

All TGases can catalyze the formation of a thioester bond between the active site Cys and the γ-carboxamide group of glutamyl substrate and ammonia is released as product. Thereafter the acyl transfer to the ε-amino group of a peptide-bound lysine residue or free amine of amine donor substrate results in the formation of the isopeptide ε-(γ-glutamyl)-lysine bond [20]. In transamidation reactions, polyamines such as spermine (SPM) or spermidine (SPD) can participate as well [33]. Besides transamidation, deamidation and isopeptide bond hydrolysis can be observed in case of different TGases [2]. In the following part, the activity and function of TG1 and TG2 is elaborated and explained.

TG1 is a Ca^{2+}-dependent enzyme involved in terminal differentiation of stratified squamous epithelia and in the formation of cornified cell envelope [34]. The cross-linking provides strength and stability to the epidermis and participates in the formation of the protective barrier between the body and environment [35]. Besides the activity and the level of TG1, Ca^{2+} treatment can increase the level of TG1 substrates and agents such as retinoic acid and phorbol esters can also influence the level of TG1 [36,37]. The TRANSDAB database contains 14 substrates for TG1 (www.genomics.dote.hu/wiki).

TG2 acts predominantly as a classic Ca^{2+}-dependent enzyme, but Ca^{2+}-independent enzymatic and non-enzymatic activities have been identified as well. TG2 as a Ca^{2+}-dependent enzyme found in several cell types and tissues has a variety of biochemical functions. It can catalyze Ca^{2+}-dependent post-translational modifications (PTMs) of proteins involving glutamine deamidation, intra- and inter protein cross-link formation and incorporation of primary amines into proteins [2]. TG2 has isopeptide bond cleavage activity [38], it can function as a protein kinase [39], can be a G protein, can bind and hydrolyze GTP [40,41] and has protein disulfide isomerase activity as well [42] (Figure 1).

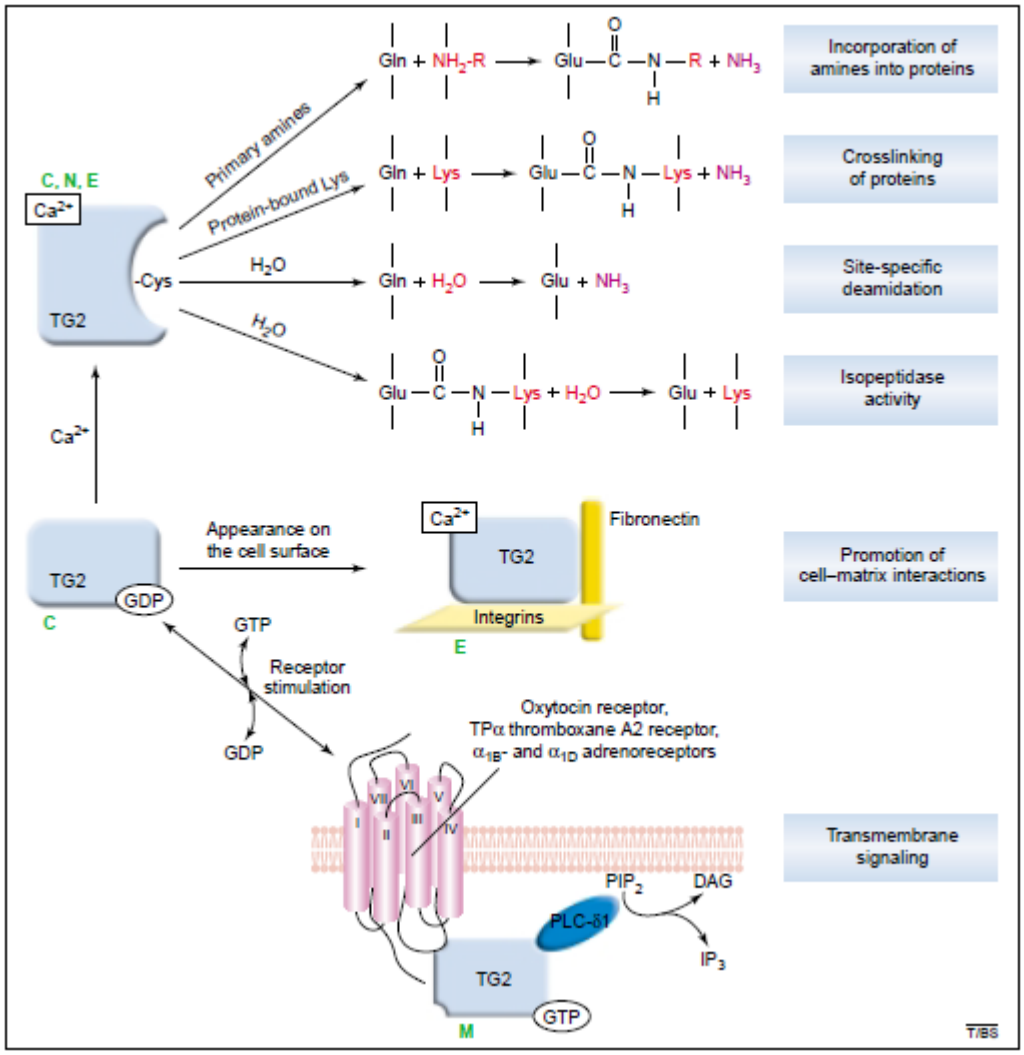

Figure 1. Reactions catalyzed by TG2 [2].

The enzymatic and non-enzymatic activities of TG2 play a role in many critical cellular processes such as cell adhesion and growth, differentiation, extracellular matrix (ECM) assembly, migration and programmed cell death [20]. It can also be present on the cell surface and in the ECM, where it cross-links and modulates several substrates such as fibrinogen, fibronectin, collagen, osteonectin, osteopontin, cell adhesion molecules, laminin-nidogen, promoting the ECM assembly and remodeling, the cell-matrix interactions providing tissue stability [43]. TG2 plays an important role in cell attachment and spreading, wound healing, promotion and inhibition of angiogenesis [17].

2.4 Transglutaminases in diseases

TGases can contribute to numerous human diseases. The activity of TG1 is dramatically reduced in lamellar ichthyosis which affects both the epidermis and hair. The symptoms of disease are erythroderma, orthokeratotic hyperkeratosis and acanthosis. In patient with this skin disorder

several mutations of the TG1 gene have been identified which is associated with deficient cross-linking of the cell envelope [16]. In *TG1* knockout mice the skin barrier function was drastically impaired and these animals died within few hours [44].

Dysfunction of TG2 is present in coeliac disease [45]; inflammatory diseases including fibrosis [46], abnormal wound healing [47] and tissue repair [48]; chronic diseases namely atherosclerosis [49], arthritis [14] and neurodegenerative conditions [50]; malignant diseases including ovarian carcinoma [51], lung carcinoma [52], pancreatic carcinoma [53], breast carcinoma [54], glioblastoma [55] and malignant melanoma [56]; metabolic diseases such as diabetes mellitus [57]. *TG2* knockout (TG2KO) mice were created by the homozygous deletion of the TG2 gene resulting in non-lethal phenotype [58]. The absence of TG2 may cause delay in wound closure that can be valuable in reducing scar formation [47,59]. In addition, TG2KO animals are viable and phenotypically (size and weight) normal, but they also carry several abnormalities in apoptosis, inflammatory and autoimmune reactions [60]. In addition, macrophages derived from TG2KO mice had impaired ability to eliminate dying cells and the different cytokines (such as interleukin-12 and transforming growth factor beta) were shown to be released by an abnormal inflammatory response [61].

2.4.1 Proliferative vitreoretinopathy

Proliferative vitreoretinopathy (PVR) is a vision-threatening disease and develops as a complication in 8-25% of patients following rhegmatogenous retinal detachment surgery [62]. PVR is characterized by intraretinal fibrosis and the formation of cellular membranes in the retina. It is a multifactorial disease caused by the interaction of various cells and intra- or extraocular factors [63]. A hallmark of PVR is the aggressive proliferation of cells including glial-, macrophage-like-, fibroblast-like- and retinal pigment epithelial cells originating from retinal breaks or holes triggering the onset of PVR [64]. This process is phenotypically similar to cutaneous wound repair. Matricellular proteins (such as thrombospondin 1 and SPARC) can modulate the activities of the cells via cell surface receptors, while the retinal pigment epithelium can remodel the new matrix via proteolytic enzymes leading to the formation of contractile scar [64]. The epithelial-to-mesenchymal transition activated by serum-derived fibronectin, platelet-derived growth factors or vitreal factors can be responsible for the formation of epiretinal membrane and hence PVR pathogenesis [65,66]. Johnsen *et al.* have shown the activation of neural progenitor cells in human PVR eyes and only the glial population near the *pars plana* region seemed to respond to retinal injury by targeted migration into the vitreous [67]. Proteolytic enzymes including thrombin [68], kininogen 1 [69] and various types of matrix metalloproteases

(MMPs) appear to play an important role in the development of PVR, and a disrupted MMP/tissue inhibitor of metalloproteinase balance was observed [70]. In animal models, the MMP effect is stimulated by the addition of dispase, a neutral Zn-metalloproteinase of bacterial origin, which can cleave various proteins that are substrates of MMPs, including collagens [71]. Johnsen *et al.* has published previously a mouse model in which the PVR induction occurs after 14 days following dispase injection [67]. The formation of new blood vessels is essential during tissue repair as well as after wound healing [72]. TG2 has been shown to directly contribute to the angiogenic response in rat dermal would healing [73] and regulate cell adhesion and migration of human corneal epithelial cells [59]. Additionally, TG2 is known to be present in human PVR membranes where it can form irreversible cross-links between ECM components leading to the tissue stabilization [74], but its exact role has not been clarified yet.

2.5 NET formation upon different factors

Human neutrophils constitute an important part of the immune system necessary to sense and control the different microbial infections [75]. They act as professional phagocytes recruited from the bloodstream and migrate to the site of infection in response to the microbial invasion. They are able to attack pathogens directly in different ways: phagocytosis, release of antimicrobial peptides and neutrophil extracellular trap (NET) formation in a process called netosis [76]. The process of NET generation is a unique type of cell death in which neutrophils eject their mixture of nucleoplasm and cytoplasm components into the extracellular space forming a web-like structure [77]. The NETs contain many forms of histones (H1, H2A, H2B, H3 and H4) as well as several antimicrobial proteins, such as azurocidin, lactoferrin, lysozyme (LYS) and cytosolic calprotectin protein complex. Proteases such as the cathepsin G (CTSG), myeloperoxidase (MPO) and neutrophil elastase (ELANE) are important constituents of the NET contributing not only to the direct microbicidal activity but also participating in microbe proteolysis [78,79] (Figure 2).

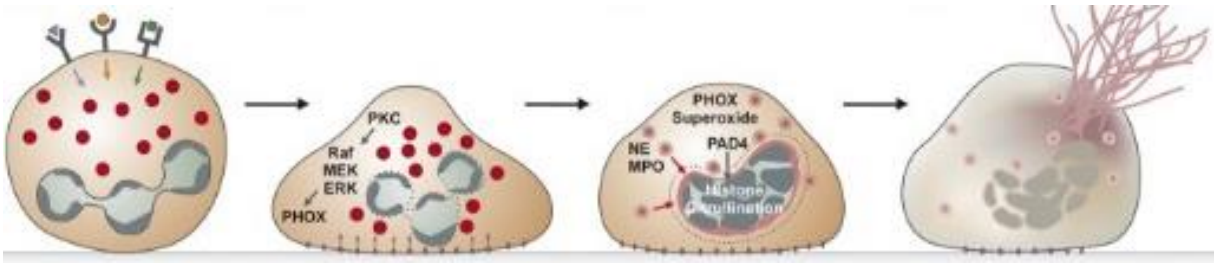

Figure 2. Schematic illustration of the NET formation [80].

Chemical and microbial factors can stimulate NETs formation resulting in dramatic changes in the morphology of neutrophils and netosis [81]. The main function of NETs is trapping and killing

almost all types of pathogens, from gram-negative and gram-positive bacteria to fungi and viruses [82]. Stimulation of neutrophil receptors leads to the attachment of neutrophils to the pathogen and chromatin decondensation occurs [80]. This process is mediated by antimicrobial enzymes ELANE, MPO, CTSG and LYS stored in azurophilic granules [79,83]. Normal neutrophil function is impaired in the absence of these proteins leading to diminished resistance to toxic agents [84–86].

One of the most frequent chemical factors activating NETs formation is phorbol-12-myristate-13-acetate (PMA) which is a protein kinase C agonist. It can activate NADPH-oxidase resulting in the formation of chromatin extracellular fibers and release of granular proteins [87]. Parker *et al.* have shown that NADPH oxidase activity is required along with PMA or bacterial stimulation. MPO is required for effective NET formation with PMA, but infection with bacteria induced NET independently of MPO activity [88].

2.6 Two-dimension gel electrophoresis and mass spectrometry in proteomics

Proteomics can help to understand the mechanism of cellular-, regulatory- and pathogenic processes, to screen the proteins of a cell, tissue or biological fluid and to identify and characterize the proteins [89,90]. The biologically active proteins are often formed by post-translational modifications. The heterogeneity of proteins makes difficult to analyze the complex biological samples. The amount of sample influences the applied method for protein analysis. Therefore, a generally applicable method for sample preparation and investigational strategy is hard to establish.

Two strategies, termed ‘bottom-up’ and ‘top-down’ proteomics, can be used to characterize proteins. During bottom-up proteomics, proteins are characterized by the analysis of peptides released from proteolytic digestion of complex samples. When the peptide mixture is fragmented and subjected to LC-MS/MS analysis, it is called shotgun proteomics [91]. It is widely used for many different research experiments such as protein identification, proteome profiling [92], protein quantification [93], protein modification detection [94] and protein-protein interaction examination [95]. Peptide identification is performed by comparing the MS/MS spectra from peptide fragmentation with the theoretical spectra generated by the search engines using the sequence information deposited in databases. Another strategy, the top-down proteomics was used for the determination of PTMs and examination of protein isoforms [96,97].

Two-dimension gel electrophoresis is a standard, high resolution method which is utilized for the analysis of proteomes of cells, tissues or other biological samples [98]. Proteins are first solubilized in a denaturing buffer containing detergent, reducing and chaotropic agents. During the first

dimension, the isoelectric focusing (IEF), proteins are separated on the basis of their isoelectric point. Then proteins are equilibrated in order to ensure the reduction of disulfide bonds and alkylation of Cys residues. During the second dimension, proteins are separated by their molecular weights (MW). All proteins have a unique IEF/MW coordinate thereby the separation of protein spots can give reliable and reproducible results [99]. Proteins can be detected usually by staining; the most commonly used stains are Coomassie-, silver- and fluorescent staining. After staining proteome changes are investigated by gel image analyzes [100]. Protein spots showing significantly changed expression are excised and identified by mass spectrometry analysis [101].
The major advantages of 2-DE in proteomics is the robustness; this is a powerful and widely used method making possible the comparison of protein profiles generated as a response to various conditions [98]. It is highly sensitive to several interfering compounds present in complex biological samples thus careful sample preparation is required [102].
2-DE was effectively applied for the examination of proteomic changes of various types of samples; retinal, muscle and colorectal tissues, Candida cells and meat were studied in normal and pathological conditions and the drug effect on protein expression was examined [103–108]. 2-DE allows the study of the expression patterns of proteins offering potential insights into protein regulation, function and interactions [109].
MS is a crucial technique for almost all proteomics experiments. It allows the identification and quantitative analysis of protein as well as the examination of the protein-protein interactions and PTMs [110]. MS as a powerful analytical technique can separate gas phase ions according to their mass-to-charge (m/z) ratio and then records the relative abundance of the ions. As a result a mass spectrum of the molecule is generated [111]. The mass spectrometer has three major parts: an ion source, a mass analyzer and a detector. The molecular ions generated in the ion source can undergo fragmentation and are separated by their m/z in the mass analyzer. The basis of separation is specific for the type of analyzer applied. There are four basic types of mass analyzer: the ion trap, time-of-flight, quadrupole and Fourier transform ion cyclotron resonance analyzer [112]. These analyzers can be stand alone or put together in tandem in order to take advantage of their strengths. Ion detector registers the intensities of all ions reaching the detector [113].
The two most commonly used ionization techniques in proteomics are matrix-assisted laser desorption ionization (MALDI) [114] and electrospray ionization (ESI) [115]. MALDI and ESI are called ‘soft’ ionization techniques because only a minimal amount of analyte is fragmented during ionization. Both techniques are suitable for the ionization of small and large molecules as well as for the analysis of proteins and peptides [116]. MALDI-MS is preformed to analyze

relatively simple peptide mixtures, while ESI-MS system is preferred for the analysis of complex samples [117].

3. Aims of the study

1. Investigation of the dispase-induced wild-type (WT) and TG2 knock-out (TG2KO) mice models of PVR in order to get information how the protein profiles are changed in PVR using two dimensional electrophoresis and mass spectrometry.

- identification of proteins with significantly changed amount upon dispase treatment in WT and TG2KO mice
- examination of protein profile changes in the lack of TG2
- study of the network of proteins changed during PVR induction in WT and TG2KO mice

2. Proteomic analysis of the NET components in order to get insights on the types of cross-links present among NET proteins

- examination of cross-links of NET proteins through chlorinated polyamines
- study of cross-links of NET proteins through ε-(γ-glutamyl)-lysine and bis-γ-glutamyl polyamine bonds catalyzed by TGases
- identification of the NET proteins and network of cross-links upon 5-(biotinamido)pentylamine and spermine treatments

4. Materials and Methods

Each chemical used for 2-DE and MS were of electrophoresis or LC-MS grade and were purchased from Sigma-Aldrich unless stated otherwise.

4.1 Animal model of PVR

The animal experiments were performed according to the ARVO Statement for the Use of Animals in Ophthalmic and Vision Research and protocols were approved by the Animal Care Committee of the University of Debrecen. Female 4-6 months old WT (C57/BL6, n = 6) and TG2KO mice (n = 6) were anesthetized with pentobarbital (90 mg kg^{-1}, i.p.), and received one drop of 1 % procaine hydrochloride (EGIS, Hungary) for local anesthesia as well as one drop of tropicamide (MYDRUM, France) for iris dilation. PVR was induced in the mice by applying an intravitreal injection of a proteolytic enzyme dispase. In these cases 4 µl dispase (0.4 U/µl, dissolved in sterile physiological saline) was injected intravitreally into the right eyes under stereomicroscopic control with an automatic pipette (fitted with 30G 1/6 needle), as previously described [118]. Into the eyes of the control animals 4 µl of sterile physiological saline solution was injected using the same procedure as for dispase injection. Following injections Stratus Optical Coherence tomography (OCT) images (Carl Zeiss Meditec, USA) were taken to confirm PVR induction. Both the control and dispase-treated mice were sacrified at 14th day following injections when signs of PVR formation such as presence of epiretinal membrane and/or retinal detachment were noticed by OCT examination.

4.2 The preparation of vitreous bodies and protein purification

The eyes of the sacrificed mice were removed and after removal of the lens and of the cornea together with a scleral galler using scalpel blade, the vitreous bodies of mice were prepared. The vitreous bodies were solubilized using lysis buffer containing 7 M urea, 30 mM Tris (pH = 8.5), 2 M thiourea and 4 % CHAPS, were sonicated in water-bath sonicator (Branson 2510) in ice cold water for 5 min and centrifuged at 16.9 g for 10 minutes at 4°C. The supernatants were transferred to LoBind Eppendorf tubes and were purified by Ready-Prep 2-D CleanUp Kit (Bio-Rad, USA) according to the manufacturer's protocol (http://www.bio-rad.com). After precipitation and centrifugation, the pellets were dried and resuspended in 450 µl rehydration buffer (7 M urea, 2 M thiourea, 4 m/V % CHAPS, 1 % dithiothreitol (DTT), 2 V/V % Bio-Lyte (Bio-Rad, USA) and 0.001 % bromophenol blue) and used immediately for IEF.

4.3 Two-dimension gel electrophoresis

Vitreal samples originating from the following groups were subjected to 2-DE: (1) dispase-treated WT (WT PVR), (2) physiological saline-treated WT (WT Ctrl), (3) dispase-treated TG2KO (TG2KO PVR) and (4) physiological saline-treated TG2KO (TG2KO Ctrl). Three biological replicates were used in each case. 24 cm IPG strips with immobilized pH gradient (pH 3-10; Bio-Rad, USA) were passively rehydrated with the extracted vitreous proteins at 20°C overnight. IEF was performed by applying 300 V for 3 hours, gradually increased to 3500 V in 5 hours and then held at 3500 V for 18 hours. The maximum current applied was 50 μA per gel. Then the IPG strips were equilibrated for 15 min in equilibration buffer (500 mM Tris-HCl, pH = 8.5, 6 M urea, 2 % SDS, 20 % glycerol) containing 0.6 % DTT and and then in equilibration buffer containing 1.2 % iodoacetamide (IAA) for 15 min. During the second dimension the strips were laid on the top of 12 % SDS-polyacrylamide gels and covered with agarose (Bio-Rad, USA). Using a Protean Plus Dodeca Cell (Bio-Rad, USA) all 12 gels were run together with 100 mA per gel for 24 hours until the bromophenol blue dye reached the bottom of the gel. The gels were pre-fixed in 10 % acetic acid, 50 % methanol and then stained with in-house prepared RuBPS fluorescent dye in 20 % ethanol overnight [119]. After staining the gels were washed and post-fixed in 7 % acetic acid, 10 % methanol. Gel images were scanned using Pharos FX Plus Molecular Imager (Bio-Rad, USA). For excitation 532 nm wavelenght light was applied and the image was recorded at 615 nm; the scanning was carried out at 100 micrometers resolution.

4.4 Image analysis using Delta2D software

Gel images were evaluated using Delta2D (Decodon) software version 4.4. The gel images were grouped as follows: (1) WT PVR, (2) WT Ctrl, (3) TG2KO PVR and (4) TG2KO Ctrl. Due to some technical problems less than 80 spots could be detected on one of the gels from the TG2KO Ctrl group, so it was excluded. In this way each group, except TG2KO Ctrl contained 3 gel images. In order to study pairwise differences between groups three projects were created: in the first project, the WT Ctrl and WT PVR gel images were studied, while in the second project the TG2KO Ctrl and TG2KO PVR gel images were examined and in the third project the WT PVR and TG2KO PVR gel images were compared.

Protein spots from each group were matched using the exact mode matching protocol and the group warping strategy of Delta2D software. The union mode was applied to generate a fused image containing all spots present on all of the gels. Every spot was quantified and the total quantity of the spots was considered as 100 %. The spot intensity was normalized according to the

total intensity of each spot in every gel and was given as normalized spot volume compared to the total intensity. The fold change of mean normalized spot volume was calculated between groups and the significant differences were assessed by the Delta2D software using Student's t-test. Those spots were considered significantly different, where the p was < 0.05. The Quantitation table generated automatically by the software was exported to Excel (Microsoft Inc.) and used for table and figure generation. Spots showing statistically significant differences were cut out for MS analysis.

4.5 In-gel digestion

The gel pieces were destained in 50% acetonitrile in 25 mM ammonium bicarbonate pH=8.5 solution, followed by reduction of disulfide bonds using 20 mM DTT (Bio-Rad, USA) for 1 hour at 56°C. Next alkylation of Cys residues was performed with 55 mM IAA (Bio-Rad, USA) for 45 min at room temperature (RT) in the dark then an overnight digestion with 100 ng stabilized MS grade trypsin (ABSciex, USA) at 37°C was accomplished. The reaction was stopped with concentrated formic acid (FA) (VWR, Hungary) and the tryptic peptides were extracted from the gel pieces and dried in speed-vac concentrator (Thermo Fisher Scientific, USA). Samples were redissolved in 10 µl 1 % FA and used for MS-based protein identification.

4.6 Protein identification by mass spectrometry

For protein identification the peptides were separated on Easy nLCII (Bruker, Germany) nanoHPLC. The chromatographic separation was performed using a 90 min water/acetonitrile gradient at 300 nl/min flow rate. The peptide mixture was loaded onto a Zorbax 300SB-C18 desalting column (5 mm x 0.3 mm, 5 µm particle size, Agilent, USA), followed by separation on a 150 mm x 75 µm Zorbax 300SB-C18 analytical column (3.5 µm particle size, 300 Å pore size, Agilent, USA). The mobile phase A was 0.1 % FA in LC-MS grade water, while the mobile phase B was acetonitrile containing 0.1 % FA. During the separation the percentage of phase B was increased from 0 % to 100 % in 60 min, then held at 100 % for 10 min, decreased to 0 % in 2 min, and finally was held at 0 % for 18 min.

The peptides eluted from the analytical column were analyzed in a 4000 QTRAP (ABSciex, USA) mass spectrometer operated by Analyst software 1.4.2 (ABSciex, USA). The positive ion mode MS/MS spectra and the Information Dependent Acquisition method was applied. The first mass scan was among 400 – 1700 amu, than an enhanced resolution scan was carried out to establish the charge state of the two most intensive precursor ions. For protein identification collision-induced dissociation spectra were obtained in enhanced product-ion mode (mass range 100 – 1900

amu) at scan rate of 4000 amu/sec and the rolling collision energy was applied with the maximum of 85 eV. The cycle time was 5.4 sec, the spray voltage was 2800 V, ion source gas was 50 pound per square inch (psi), the curtain gas was 20 psi and the source temperature was 70°C. Based on the recorded MS/MS spectra proteins were identified with the ProteinPilot 4.5 software (ABSciex, USA) using the UniProtKB/Swiss-Prot database. The minimum criteria for protein identification were the presence of two peptides per protein with at least 95 % confidence. In those cases where the protein identification was not successful using ProteinPilot software, a MASCOT search was carried out using the NCBInr database. The type of cleavage enzyme was defined as trypsin. The missed cleavage in all cases was set to maximum 1. In case of MASCOT search the variable modifications were set as: oxidation of methionine (Met) and carbamidomethylation of Cys, while in case of ProteinPilot 4.5 (ABSciex, USA) search the Biological modification table implemented into the software was applied.

4.7 Functional analysis of proteomics changes

The gene ontology (GO) analysis was used for the functional analysis of the proteins [120]. The Biological Process, Molecular Function and Cellular Localization according to GO was examined using String version 10.5 [121]. The network of differentially expressed proteins along with GO enrichment data was generated.

4.8 Isolation of neutrophils from human venous blood

50 ml of human venous blood from healthy volunteers was collected into vacutainer tubes containing EDTA (BD, 367525) and centrifuged for 15 min, at 500 g on RT in order to remove plasma containing thrombocytes [122]. Ethical approval was obtained from the Ethics Committee of the University of Debrecen, Debrecen, Hungary (DEOEC RKEB/IKEB Prot. No. 2745-2008). Cells were transferred into 50 ml tube and 12 ml 3 % dextran (Dextran T500, Pharmacocosmos, Denmark) in physiological saline solution (sterilized using 0.22 μm filter, TPP Spritzen) was added to the cells. Then the tube was filled up to 50 ml with physiological saline solution and incubated for 30 min on RT. After floating foam containing red blood cells was removed, supernatant containing white blood cells was collected and diluted 4 times with 20 mM PBS-EDTA in 15 ml tube. Cells were centrifuged for 7 min, at 300 g on RT. After supernatant was discarded, pellet was suspended in 3 ml 20 mM PBS-EDTA and cells were layered on Histopaque gradient (6 ml Hp 1119, 5 ml Hp 1077) and then centrifuged for 30 min, at 300 g on RT. Supernatant (containing lymphocytes and monocytes) was removed and neutrophils were collected into 50 ml tube and washed 2 times with 50 ml 20 mM PBS-EDTA. After centrifugation for 7 min, at 300 g on RT,

the rest of the thrombocytes was removed and cells were suspended in 30 ml RPMI 1640 medium containing 1% penicillin-streptomycin, 1% L-glutamine, 1% pyruvate. Cells were centrifuged again for 7 min, at 300 g on RT, supernatant was removed and cells were suspended in 1 ml RPMI 1640 medium. The cells were counted, NET was induced and used either for protein isolation or fluorescent microscopy.

4.9 Purification of NET proteins

2 x 10^6 neutrophils were seeded in 6-well tissue culture plates in 4 ml RPMI 1640 medium. Neutrophils were pre-incubated with RPMI 1640 medium (Ctrl) or 0.5 mM 5-(biotinamido)pentylamine ($BPNH_2$) or SPM, then activated with 20 nM PMA for 4 h at 37°C in a 5% CO_2 atmosphere [123].

After removing the medium, all wells were carefully washed by pipetting 1 ml of fresh and pre-warmed RPMI 1640 medium containing protease inhibitor cocktail and incubated for 10 min at 37°C. The medium was removed, the formed NETs were digested for 20 min in 1 ml fresh RPMI medium with 10 Unit/ml DNase-1 (Worthington, USA), followed by centrifugation at 16.9 g at 4°C. To precipitate the proteins 0.5 ml of supernatant was mixed with 1.5 ml of ice-cold acetone and incubated overnight at -20°C. Samples were centrifuged at 10.4 g for 30 min at 4°C. Then pellets were solubilized in 200 µl Laemmli buffer and frozen at -70°C for further analysis.

4.10 SDS-polyacrylamide gel electrophoresis

Total concentration of NET proteins was determined with Bradford assay [124]. In all cases 20 µg NET protein was separated on 12% polyacrylamide gel in a Mini Protean Tetra Cell (Bio-Rad, USA). Electrophoresis was carried out for 1.5 hours at 30 mA constant current and ProSieve™ Protein Ladder (Lonza, Switzerland) as a protein MW marker was used. Protein staining was performed by PageBlue™ Protein Staining Solution (Thermo Fisher Scientific, USA), gels were scanned using Pharos FX Plus Molecular Imager (Bio-Rad, USA) and the gel image analysis was carried out by QuantityOne Software (Bio-Rad, USA). The band intensities and the estimated MW for each band was calculated.

4.11 MS/MS based investigation of cross-linked NET proteins using StavroX software

StavroX 3.2.10 software was applied to identify possible cross-links among the NET proteins [125]. The MS/MS data in Mascot generic format (.mgf) including all recorded spectra were used for the analyses. Amino acid sequences of the previously identified NET proteins were imported from UniProtKB in FASTA format. Enzymatic cleavage sites of trypsin were defined as C-

terminal to Lys and arginine and blocked by proline. Variable modifications were set as oxidation of Met and carbamidomethylation of Cys. SPM, SPD and putrescine (PUT) were applied as probable cross-linkers, searching for the presence of the following cross-links: 1) Lys-polyamine-Lys cross-links with 200 Da, 143 Da and 86 Da mass shift for SPM, SPD and PUT incorporation, respectively, 2) Lys-polyamine-Met cross-links with 200 Da, 143 Da and 86 Da mass shift for SPM, SPD and PUT incorporation, respectively, 3) Gln-polyamine-Gln cross-links with 166 Da, 109 Da and 54 Da mass shift for SPM, SPD and PUT incorporation, respectively, and 4) Gln-Lys cross-links with 17 Da mass shift. The calculated mass shifts were implemented into the software and the MS/MS spectra were searched for b- and y- ions corresponding to all possible cross-links. The results were manually analyzed and those hits were accepted where the score value of the identified cross-linked proteins was positive and contained at least four ions of b- or y-ion in series. The sequence of the cross-linked peptides and the position of the cross-link was imported to Excel files and utilized for the visualization of the network of cross-linked NET proteins.

5. Results

TGases can catalyze a vast array of protein post-translation modifications including protein-protein crosslinking, incorporation of primary amines into proteins in a calcium-dependent reaction [1]. The crosslinked protein products are more resistant to proteolytic degradation and mechanical challenge [2]. TGases can exert their functions by modifying substrates and binding to interaction partners. TRANSDAB database consists more than 500 transglutaminase substrate proteins and interaction partners [32].

5.1 Examination of protein profile changes in dispase-induced model of proliferative vitreoretinopathy

The specific proteins involved in the pathogenesis of PVR and the effect of TG2 on PVR formation were studied in mice using WT and TG2KO animal models. In both setups, the PVR was induced by the addition of dispase and the differences in protein expression were studied between the groups. By comparing the WT Ctrl versus WT PVR group, our aim was to obtain information on the proteins which participate in the PVR pathogenesis. Concerning the role of TG2 which is not known precisely in PVR, the differentially expressed proteins between TG2KO Ctrl and TG2KO PVR groups were examined with the aim to identify proteins which might be related to TG2 and respond with altered expression for the combined effect of absence of TG2 and induction of PVR. Meanwhile, an attempt was made to identify the proteins which are TG2-dependent in PVR by comparing the WT PVR and the TG2KO PVR groups.

5.1.1 Proteins characteristic for PVR induction by dispase treatment in wild type mice

Dispase treated WT mice were used to examine protein changes in PVR. 2-DE was performed on 3 Ctrl and 3 dispase-treated WT mice vitreous. Gels were stained using RuBPS [119] and the gel images were scanned and analyzed by Delta2D (Decodon) software. The WT Ctrl group was created from the 3 gel images originating from physiological saline-treated samples, while the WT PVR group was made up of 3 gel images originating from dispase-treated samples. A fused image was generated by superimposing each gel image and 698 spots could be detected (Figure 3).

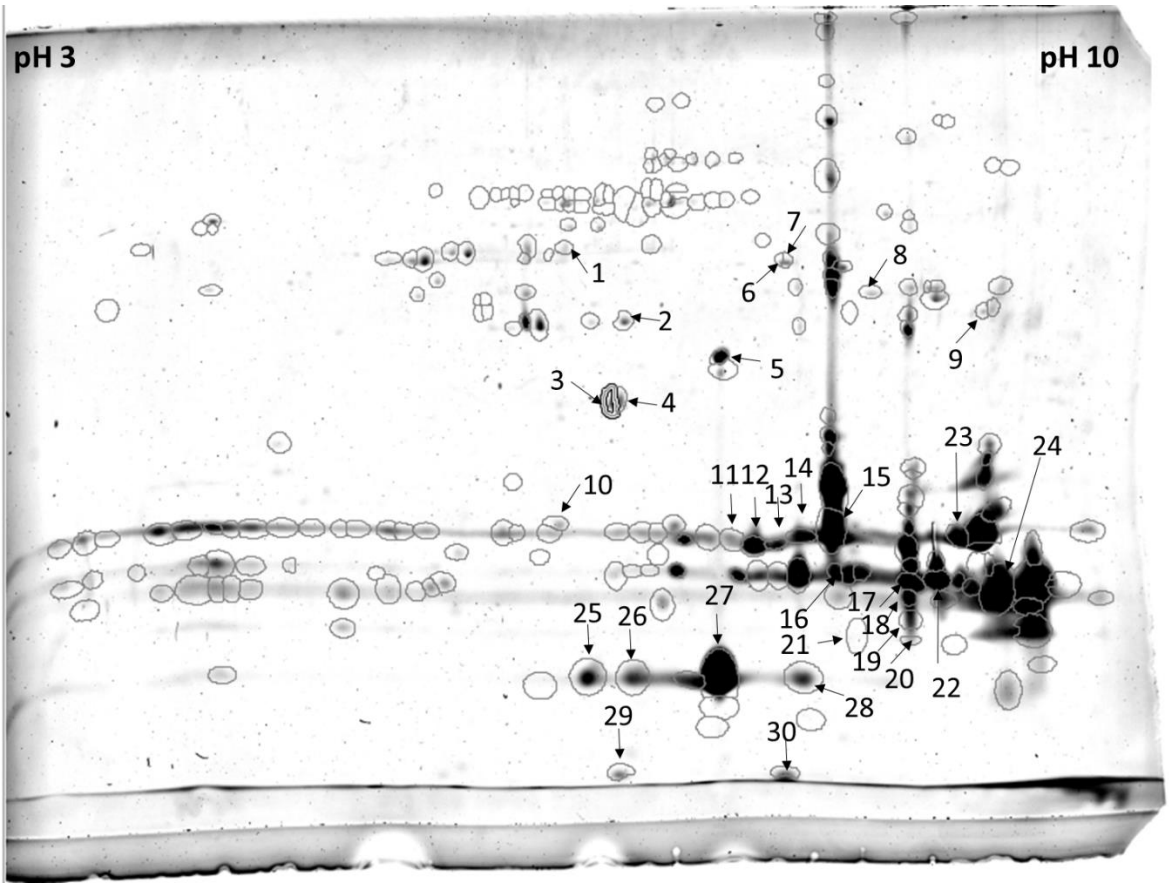

Figure 3. Fused image originating from the superposition of WT Ctrl and WT PVR gel images by Delta2D software. *The numbered spots are those ones which show significantly different intensities between groups.*

In case of each gel the intensity of all spots was determined and the fold change between the groups was calculated. The intensity of 30 out of 698 spots indicated significant ($p < 0.05$) changes as an effect of dispase treatment and these 30 spots were excised from the gel, digested by trypsin and subjected to HPLC-MS/MS-based protein identification (Table 2).

Spot ID	Protein ID	Protein name	Number of peptides	Fold change	p value
1	P99024	Tubulin beta-5 chain	6	- 0.23	0.03
2	Q04447	Creatine kinase B-type	15	- 0.27	0.03
3	P62874	Guanine nucleotide-binding protein G(I)/G(S)/G(T) subunit beta-1	11	- 0.11	0.02
4	P62874	Guanine nucleotide-binding protein G(I)/G(S)/G(T) subunit beta-1	8	- 0.08	0.03
5	P24622	Alpha-crystallin A chain	7	- 0.23	0.02
6	O35737	Heterogeneous nuclear ribonucleoprotein H	4	- 0.09	0.049
7	O35737	Heterogeneous nuclear ribonucleoprotein H	3	- 0.11	0.04
8	P17182	Alpha-enolase	11	- 0.21	0.049
9	P15105	Glutamine synthetase	8	- 0.41	0.049
10	P14602	Heat shock protein beta-1	5	- 0.32	0.02
11	P02525	Beta-crystallin A1	3	- 0.17	0.01
	P62696	Beta-crystallin B2	3		
12	P02525	Beta-crystallin A1	3	- 0.37	0.046
	P62696	Beta-crystallin B2	3		
13	P62696	Beta-crystallin B2	4	- 0.46	0.01
	P02525	Beta-crystallin A1	3		
	Q9JJV1	Beta-crystallin A2	2		
14	P02525	Beta-crystallin A1	3	- 0.37	0.04
	P62696	Beta-crystallin B2	3		
15	P02525	Beta-crystallin A1	4	- 0.41	0.01
16	P24622	Alpha-crystallin A chain	7	- 0.51	0.02
	Q9JJV1	Beta-crystallin A2	4		
17	P24622	Alpha-crystallin A chain	8	- 0.50	0.001
	P02525	Beta-crystallin A1	5		
18	P02525	Beta-crystallin A1	5	- 0.32	0.04
	P24622	Alpha-crystallin A chain	4		
19	P02525	Beta-crystallin A1	3	- 0.25	0.01
20	P02525	Beta-crystallin A1	3	- 0.11	0.03
21	P23927	Alpha-crystallin B chain	2	0.27	0.02
22	O35486	Beta-crystallin S	2	- 0.34	0.01
	P04344	Gamma-crystallin B	2		
23	P62696	Beta-crystallin B2	7	- 0.36	0.0002
24	P2392	Alpha-crystallin B chain	8	- 0.44	0.03
	O35486	Beta-crystallin S	7		
	Q61597	Gamma-crystallin C	5		
25	P24622	Alpha-crystallin A chain	9	- 0.47	0.03
26	P24622	Alpha-crystallin A chain	9	- 0.28	0.02
27	P24622	Alpha-crystallin A chain	10	- 0.49	0.02
28	P24622	Alpha-crystallin A chain	10	- 0.25	0.02
29	Q9D1U0	Grifin	3	- 0.53	0.003
30	Q05816	Fatty acid-binding protein, epidermal	4	- 0.25	0.004

Table 2. List of identified proteins in spots showing significantly different intensity upon dispase treatment. *The spot number, the Uniprot code, protein name, the number of unique peptides achieved by MS/MS analysis, the fold change value (WT PVR vs. WT Ctrl) and significance levels are shown.*

In case of 19 spots, different forms of crystallins were identified. Crystallins are known as stress proteins with three main types: α, ß, and γ [126]. 8 out of 19 spots contained alpha-crystallin A and the amount of different forms of crystallins (except alpha-crystallin B) was reduced. The

expression level of intracellular proteins such as alpha-enolase, creatine kinase B-type, Gln synthetase, G protein, grifin, heat shock protein beta-1, heterogeneous nuclear ribonucleoprotein H, fatty-acid binding protein 5 and tubulin decreased in the dispase-treated WT samples compared to the physiological saline treated ones (Table 2).

In case of spots 11-14, 16-18, 22 and 24 more than one protein with similar peptide counts was detected. The combined effect of these proteins could be observed in such cases, therefore there is no information about the spot intensity changes of each individual protein.

5.1.2 Proteins characteristic for PVR induction by dispase treatment in TG2KO mice

Mice models are used to examine the function of proteins as far as the KO animals for the protein of interest can easily be created. TG2 is a multifunctional enzyme having various roles in physiological and pathological conditions [2]. It was shown that TG2 is present in PVR membranes [74], but its role in PVR has not been examined in details. In order to present the feasibility of the mice PVR model in elucidating the role of TG2 in PVR, dispase and physiological saline solution, respectively was injected into the eyes of TG2KO animals. The strategy used for the investigation of WT Ctrl and WT PVR samples was applied also in case of TG2KO samples. The vitreous samples were analyzed by 2D electrophoresis followed by protein staining and image analysis. On one of the gel images from the TG2KO Ctrl group was excluded because for some technical problem less than 80 spots could be detected, so TG2KO Ctrl group contained only 2 gel images. The images from the TG2KO Ctrl and the TG2KO PVR group were superimposed to generate the fused image (Figure 4).

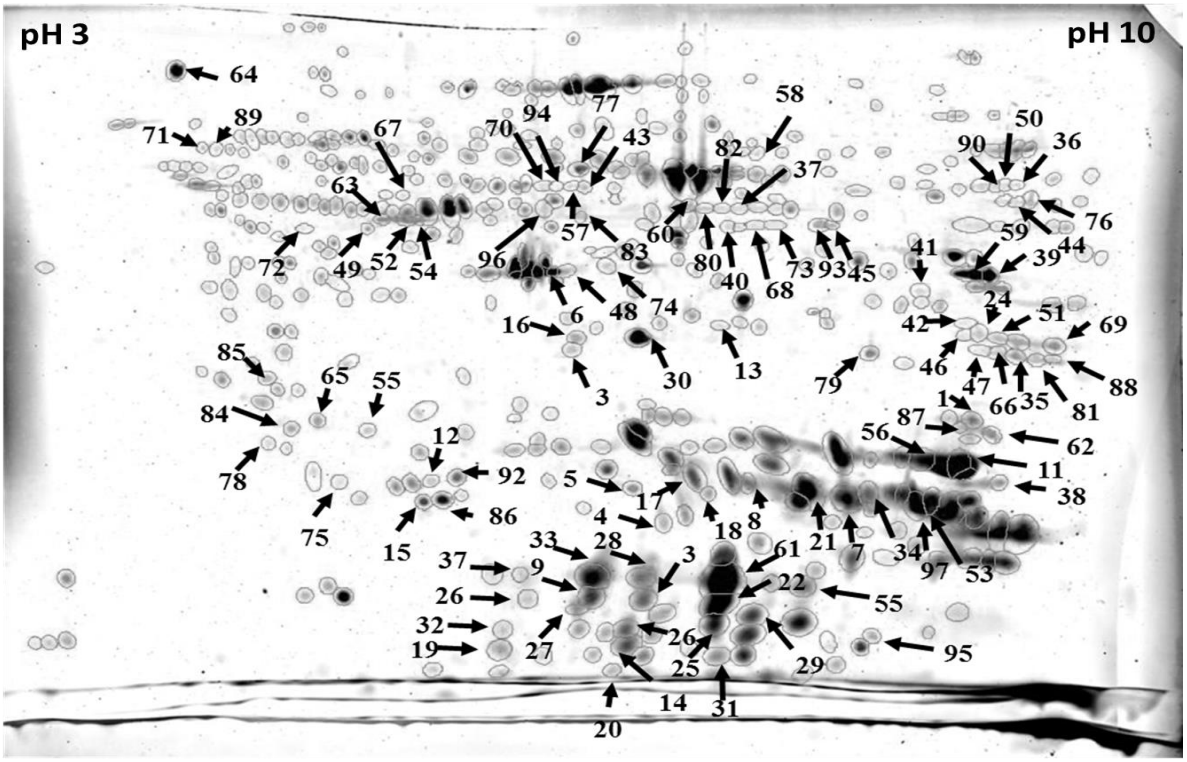

Figure 4. Fused image originating from the superposition of TG2KO Ctrl and TG2KO PVR gel images by Delta2D software. *The numbered spots are those ones which show significantly different intensities between groups.*

866 spots were detected and 97 of them showed significantly different ($p < 0.05$) changes in their intensities upon dispase treatment. The amount of proteins in 33 spots elevated, while in 64 spots reduced.

Some spots in the basic pH and lower MW region of the gels could be detected only on TG2KO PVR gels; despite of otherwise good quality of protein separation, very few spots were visible in the gel region corresponding to basic, low MW proteins in case of control samples (Figure 5).

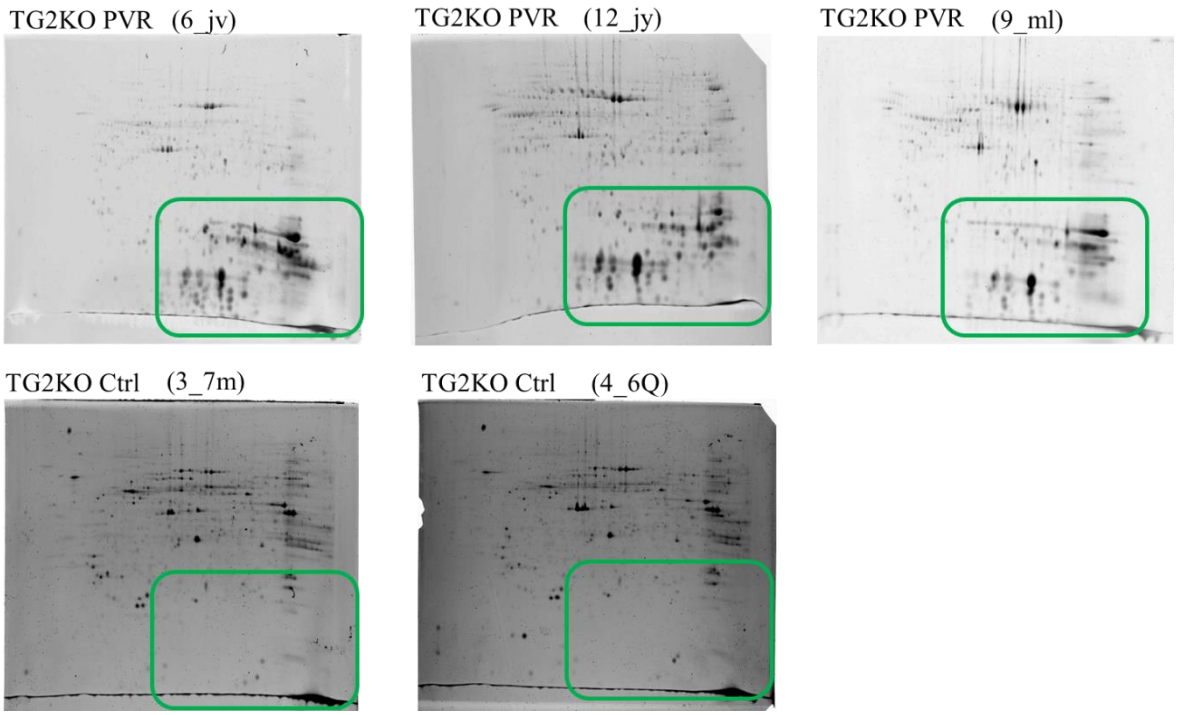

Figure 5. Images of the examined gels with highlighted basic pH and lower molecular mass region (green rectangle). *The unique identifiers of the strips are also indicated in brackets in case of each gel.*

The spots with significantly different intensity changes were cut out and 37 of them were identified with MS-based analysis. In consort with the previous results, most spots showing altered intensity changes upon dispase treatment contained alpha-crystallin, but in this case, their level was elevated upon dispase treatment (Table 3).

Spot ID	Protein ID	Protein name	Number of peptides	Fold Change	p value
1	P99024	Tubulin beta-5 chain	6	-5.57	0.003
	P68373	Tubulin alpha-1C chain	3		
3	P24622	Alpha-crystallin A chain	9	76.45	0.01
7	P70333	Heterogeneous nuclear ribonucleoprotein H2	2	-9.51	0.003
14	P09528	Ferritin heavy chain	3	5.82	0.04
15	P24622	Alpha-crystallin A chain	3	-6.28	0.005
16	Q8BFZ3	Beta-actin-like protein 2	4	-7.01	0.01
18	P02525	Beta-crystallin A1	4	41.04	0.05
19	P02525	Beta-crystallin A1	3	5.13	0.01
20	P24622	Alpha-crystallin A chain	3	49.71	0.01
26	P24622	Alpha-crystallin A chain	7	128.66	0.02
27	P02525	Beta-crystallin A1	3	4.25	0.03
31	P34057	Recoverin	2	-18.90	0.02
33	P16125	L-lactate dehydrogenase B chain	2	-7.59	0.007
34	P24622	Alpha-crystallin A chain	8	106.31	0.005
38	Q61171	Peroxiredoxin-2	3	-7.51	0.001
42	Q61838	Alpha-2-macroglobulin	2	-20.54	0.0002
44	P24622	Alpha-crystallin A chain	7	196.24	0.006
47	P29391	Ferritin light chain 1	6	56.65	0.04
48	P24622	Alpha-crystallin A chain	2	9.03	0.01
49	P24622	Alpha-crystallin A chain	3	17.14	0.02
	Q9D1U0	Grifin	2		
50	P24622	Alpha-crystallin A chain	3	8.92	0.02
51	P24622	Alpha-crystallin A chain	6	83.15	0.003
55	P24622	Alpha-crystallin A chain	4	31.65	0.03
60	P16858	Glyceraldehyde-3-phosphate dehydrogenase	3	-13.74	0.0002
64	P24622	Alpha-crystallin A chain	5	42.28	0.0005
67	P24622	Alpha-crystallin A chain	8	18.79	0.02
70	P24622	Alpha-crystallin A chain	5	22.95	0.0005
74	P24622	Alpha-crystallin A chain	5	88.39	0.03
77	P24622	Alpha-crystallin A chain	3	31.74	0.005
83	P62880	Guanine nucleotide-binding protein G(I)/G(S)/G(T) subunit beta-2	3	-16.39	0.0001
84	P24622	Alpha-crystallin A chain	5	12.72	0.01
87	P24622	Alpha-crystallin A chain	3	21.14	0.0006
88	P24622	Alpha-crystallin A chain	5	36.78	0.0007
90	P24622	Alpha-crystallin A chain	10	11.36	0.004
	P02525	Beta-crystallin A1	2		
	P35700	Peroxiredoxin-1	2		
91	P06151	L-lactate dehydrogenase A chain	2	-22.83	0.0005
94	Q921I1	Serotransferrin	3	-7.40	0.0005
96	P24622	Alpha-crystallin A chain	6	23.98	0.0002

Table 3. List of identified proteins in spots showing significantly different intensity upon dispase injection in TG2KO mice. *The spot number, the Uniprot code, protein name, the number of unique peptides achieved by MS/MS analysis, the fold change value (TG2KO PVR vs. TG2KO Ctrl) and significance levels are shown.*

The amount of a G-protein, heterogeneous nuclear ribonucleoprotein and tubulin was reduced upon dispase treatment, being in accordance with previous results obtained by the analysis of WT

mice. The amount of glycolytic enzymes glyceraldehyde-3-phosphate dehydrogenase, lactate dehydrogenase, of cytoskletal protein beta-actin-like protein 2, of recoverin, peroxiredoxin 2, serotransferrin and alpha-2 macroglobulin was reduced as well. In the same time the level of beta-crystallin A1, ferritin light and heavy chains and grifin increased in TG2KO PVR samples.

When the changes in WT and TG2KO mice in PVR were compared (Figure 6) 4 of the proteins have shown changes in both conditions. The level of tubulin beta 5 reduced upon dispase treatment both in the presence or absence of TG2. In WT PVR the level of alpha-crystallin A, beta-crystallin A1 and grifin decreased, while in TG2KO PVR an increase was observed. There was one spot containing alpha-crystallin A where reduction in the protein amount could be observed in TG2KO PVR.

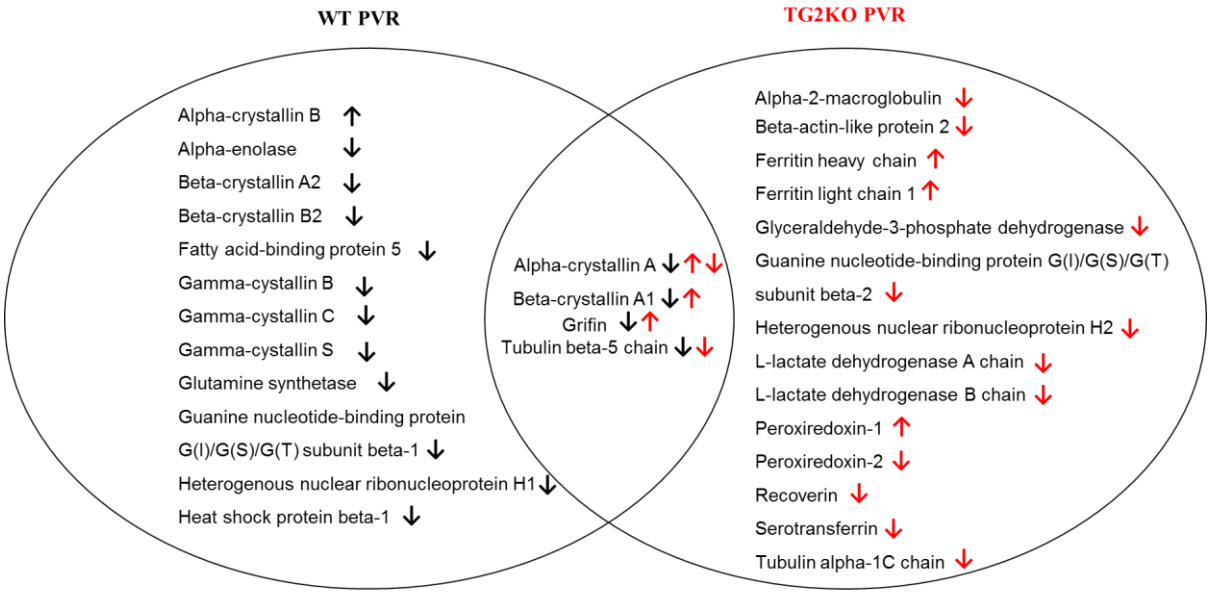

Figure 6. Protein amount changes upon dispase treatment. *Arrows show the direction of changes in WT and in TG2KO samples, respectively, upon dispase treatment, compared with the control samples. The black arrows refer to the changes in the WT mice, while the red arrows indicate the changes in the TG2KO mice upon dispase treatment.*

5.1.3 Proteins affected by the lack of TG2 in mice vitreous during PVR formation

The proteins in which the expression depends on TG2 during PVR formation were investigated by comparing gel images of WT PVR groups to TG2KO PVR groups. The only difference between the two groups was the presence or absence of TG2, and this resulted in significantly different expression in case of 41 spots (Figure 7).

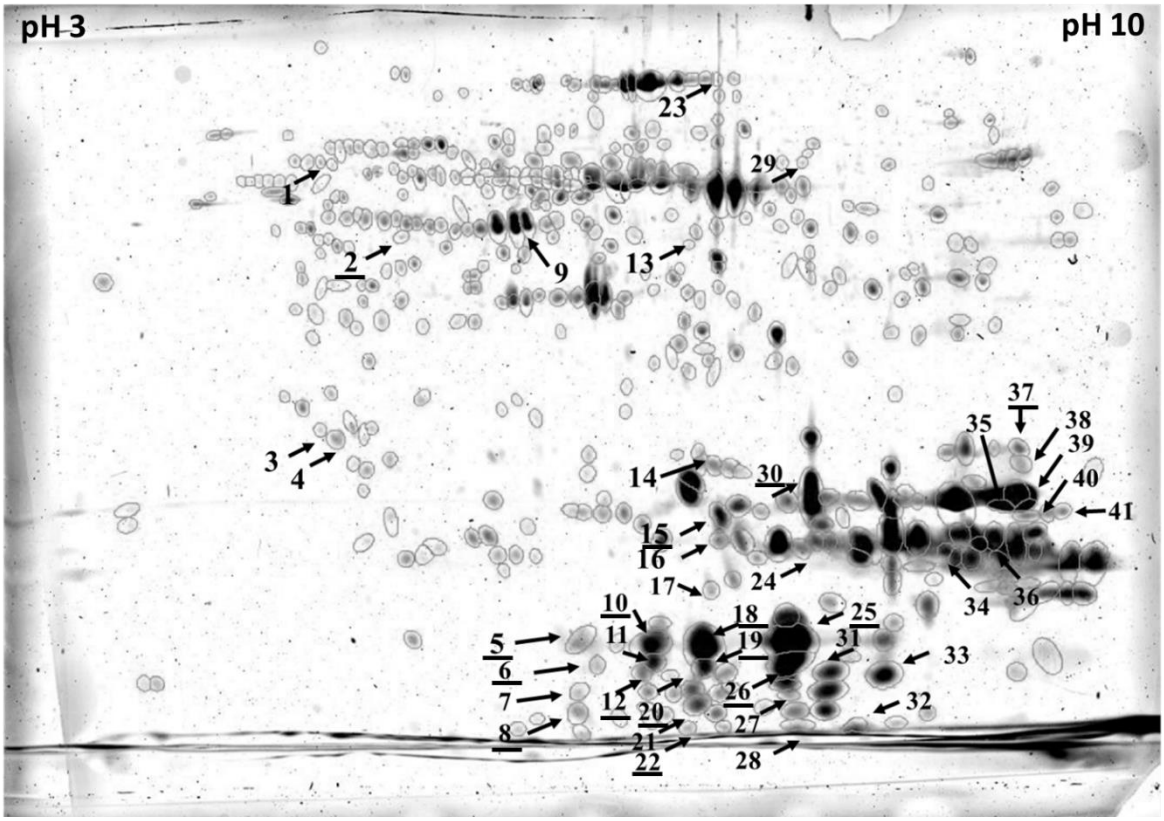

Figure 7. Fused image originating from the superposition of WT PVR and TG2KO PVR gel images by Delta2D software. *The numbered spots are those ones which show significantly different intensities between groups. The underlined spot numbers refer to spots which were identified in our previous MS/MS experiment.*

15 spots were previously identified by MS/MS; in 12 spots alpha- or beta-crystallin was present while the other 3 spots contained ferritin heavy chain, griffin and tubulin, respectively.

5.1.4 Functional analysis of proteins differentially expressed upon dispase treatment

The network of proteins showing significant changes upon dispase treatment was generated by String. In case of WT mice the network contained 17 proteins (nodes) and 14 possible protein-protein interactions analyzed at medium stringency (Figure 8A). The enriched biological and molecular functions were eye development and protein binding indicating that most of the proteins implicated in PVR development may play a role in the correct development and structural stabilization of the eye (Figure 8B).

A.

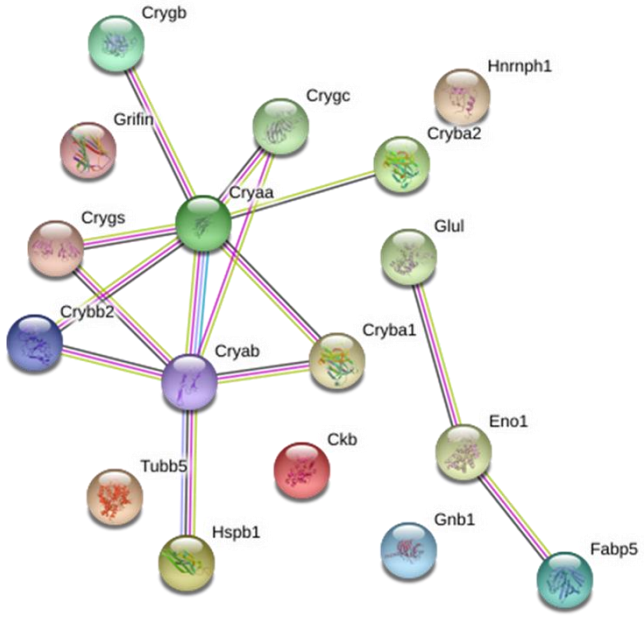

B.

Pathway ID	Pathway description	Observed gene count	False discovery rate
I. Biological process			
GO.0043010	Camera-type eye development	8	2.12e-07
GO.0002088	Lens development in camera-type eye	4	0.000485
II. Molecular Function			
GO.0005212	Structural constituent of eye lens	8	6.13e-17
GO.0042802	Identical protein binding	7	0.00538
III. Localization			
GO.0043209	Myelin sheath	5	0.000354

Figure 8. The protein-protein interaction network and functional classification of proteins in WT samples. *A. The network nodes are proteins identified by the gene name, while edges show the functional associations based on different types of evidence according to the String color coding scheme* [121]. *B. The eriched GO terms in the network calculated by String. The number of the proteins belonging to each term and the false discovery rate values are indicated.*

The network of proteins with significantly different amount in TG2KO mice contained 18 proteins (nodes) and 24 protein-protein interactions (edges) (Figure 9A). The enriched biological and molecular functions indicate active metabolic and homeostatic mechanisms involving oxidoreductase-, L-lactate dehydrogenase-, thioredoxin peroxidase activities and ferric iron binding (Figure 9B).

A.

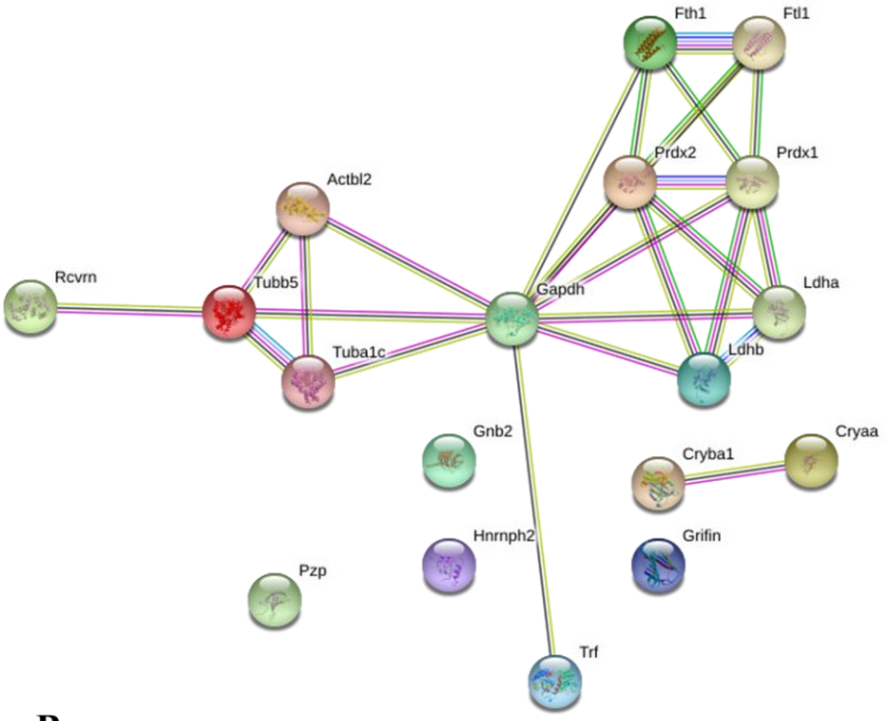

B.

Pathway ID	Pathway description	Observed gene count	False discovery rate
I. Biological process			
GO.0055114	Oxidation-reduction process	6	0.0407
GO.0006090	Pyruvate metabolic process	3	0.0303
GO.0006879	Cellular iron ion homeostasis	3	0.0243
GO.0019244	Lactate biosynthetic process from pyruvate	2	0.0243
II. Molecular Function			
GO.0016491	Oxidoreductase activity	6	0.00542
GO.0004459	L-lactate dehydrogenase activity	2	0.00241
GO.0008379	Thioredoxin peroxidase activity	2	0.00241
GO.0008199	Ferric iron binding	3	0.000143
III. Localization			
GO.0005576	Extracellular region	10	0.0213
GO.0030139	Endocytic vesicle	3	0.0195
GO.0044421	Extracellular region part	10	0.00848
GO.0031988	Membrane-bounded vesicle	10	0.00691

Figure 9. The protein-protein interaction network and functional classification of proteins in TG2KO samples. *A. The network nodes are proteins identified by the gene name, while edges show the functional associations based on different types of evidence according to the String color coding scheme* [121]. *B. The eriched GO terms in the network calculated by String. The number of the proteins belonging to each term and the false discovery rate values are indicated.*

The localization of proteins in TG2KO PVR was mostly in extracellular region and vesicles, while in case of WT mice it was mainly in myelin sheath.

5.2 Investigation of potential role of transglutaminase in neutrophil extracellular trap formation

Biochemical determinants of stable NETs have not been established so far. During the study it was observed by colleagues that endogenous polyamines as well as monoamines play a role in the formation of NET. The SPM as a polyamine was detected in association with decondensed chromatin and NET DNA filaments in activated neutrophils suggesting that SPM gets incorporated into the NET. In addition, an increase in the level of covalently bound spermine to cellular proteins in PMA stimulated neutrophils was detected. $BPNH_2$ as a potential competitive monoamine inhibitor of polyamine incorporation was used for examination of the effect of TGase on SPM incorporation. We performed the proteomic analysis of the NET components in order to see whether the exogenous SPM and $BPNH_2$ changes the protein composition of PMA activated neutrophils possibly resulting in the alteration of the stability of the NET structure.

5.2.1 Proteomic analysis of the NET components

Protein profile of the isolated NET was investigated by proteomic approach. 20 μg of isolated NET proteins of Ctrl, $BPNH_2$ and SPM-treated samples originating from three donors were separated on 12 % SDS-polyacrylamide gels (Figure 10). In case of donor 1 (D1) no SPM treatment was performed.

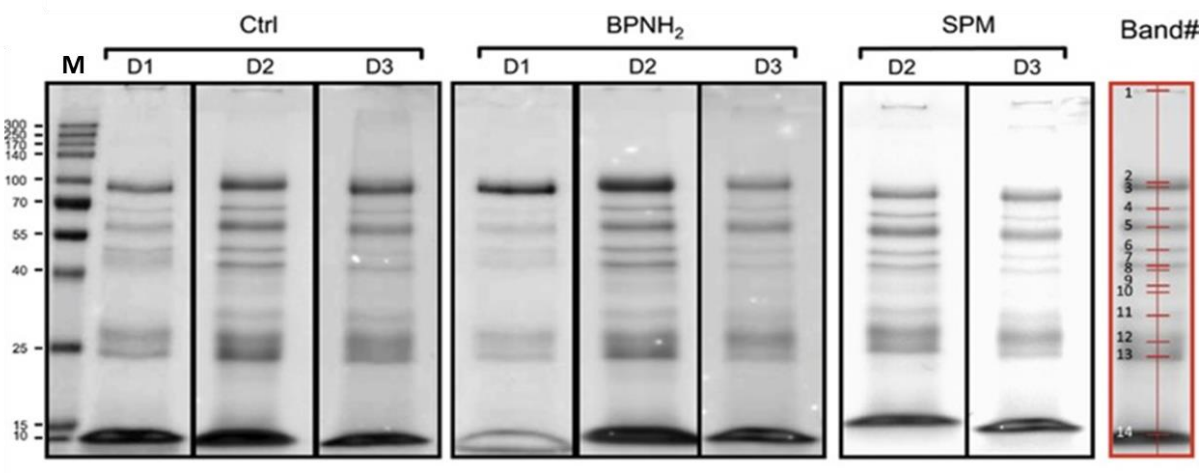

Figure 10. Proteomic analysis of Ctrl, BPNH$_2$ and SPM treated NET proteins from 3 donors (D1, D2, D3). *The detected bands and the band numbers assigned by QuantiyOne (Bio-Rad, USA) band analysis software are marked with red. The applied MW marker is indicated on the left side of the gel image.*

Gel image analysis of Ctrl, BPNH$_2$ and SPM treated NET samples was performed. We observed a highly reproducible pattern of protein bands after separation on 12% SDS-polyacrylamide gel. Alterations in band intensities upon BPNH$_2$ and SPM treatment could be observed, however the differences were not statistically significant (Figure 11).

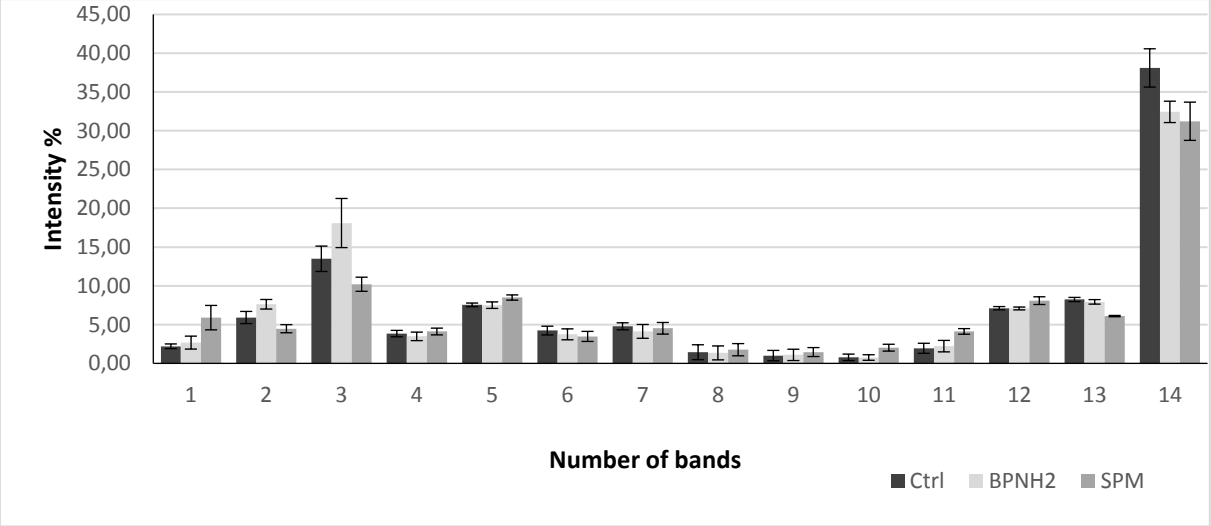

Figure 11. Band analysis of 1D gel images using QuantityOne Software. *The intensity of each band is expressed as a percentage of the total quantity of all bands in the lane.*

Bands were excised and subjected to MS/MS-based protein identification. We could identify 16 NET proteins, 14 out of them have already been published [127], while protein S100-A6 and leukocyte elastase inhibitor are novel NET proteins (Table 4). Some proteins were identified in

bands corresponding to their theoretical MW, but many of them migrated to different positions which might indicate extensive protein processing.

Band #	MW	Ctrl	$BPNH_2$	SPM
1	>300	**AZU1, ELANE, S100A8**	**ELANE**	**AZU1, ELANE**
2	98.98	**LTF**	**LTF**	**LTF**
3	87.14	LTF	LTF	LTF
4	67.13	**LTF,MPO,**TKT	**LTF**, TKT	**MPO,** TKT
5	58.19	CAT, **LTF,MPO**	CAT, **LTF,MPO**	CAT, **MPO**
6	49.14	ENO1,**LTF,MPO**	ENO1, **LTF**	ENO1,**LTF,MPO**
7	43.42	**LTF,MPO**	**LTF, SERPINB1**	**LTF,MPO**
8	40.10	**MPO**	**SERPINB1**	**SERPINB1, MPO**
9	37.69	N/D	**MPO**	**MPO, S100A8**
10	36.43	**AZU1,MPO**	**LTF,MPO**	**AZU1, MPO, LTF**
11	31.14	**AZU1, CTSG**	**AZU1, LTF**	**AZU1**
12	26.84	AZU1, CTSG, ELANE, LTF, MPO, S100A8	AZU1, CTSG, ELANE, **MPO**	AZU1, CTSG
13	24.15	**AZU1, CTSG, ELANE, LTF, MPO, S100A8**	**CTSG, ELANE, LTF, MPO**	**AZU1, CTSG, ELANE,LTF**
14	12.10	**AZU1, CTSG, ELANE, LTF, LYZ, MPO**, HIST1H2B, HIST1H4, **S100A6**, S100A8, S100A9	**AZU1, CTSG, ELANE, LTF, LYZ, MPO**, HIST1H2A, HISTH1H2B, HIST1H4, S100A8, S100A9	**AZU1, CTSG, LYS, MPO**, HIST1H2A, HISTH2B, HIST1H3, S100A8, S100A9

Table 4. List of NET proteins identified in Ctrl, $BPNH_2$ and SPM treated samples using LC-MS/MS-based mass spectrometry analysis. *The proteins in the table are represented by their Uniprot gene name. The band number and the estimated MW value for each band is indicated. Bold face indicates the presence of proteins at different MWs than expected.*

5.2.2 Investigation of polyamines mediated protein cross-links by chlorinated polyamines and transglutaminase reaction

In order to detect the presence of potential cross-links formed between the identified proteins, the MS data were analyzed by StavroX [125]. The presence of four possible cross-links were examined. Chloramines of SPM, SPD and PUT can be formed upon the MPO activity [128]. The chloramines can react with protein-bound lysines or methionines resulting in Lys-polyamine-Lys or Lys-polyamine-Met cross-links [129]. SPM, SPD and PUT can form cross-links between protein-bound glutamines in a reaction catalyzed by the TGase as well [33]. Beside this, TGases are able to catalyze the formation of isopeptide bonds between protein-bound Lys and Gln, therefore the presence of γ-Gln-ε-Lys cross-links was also monitored (Figure 12).

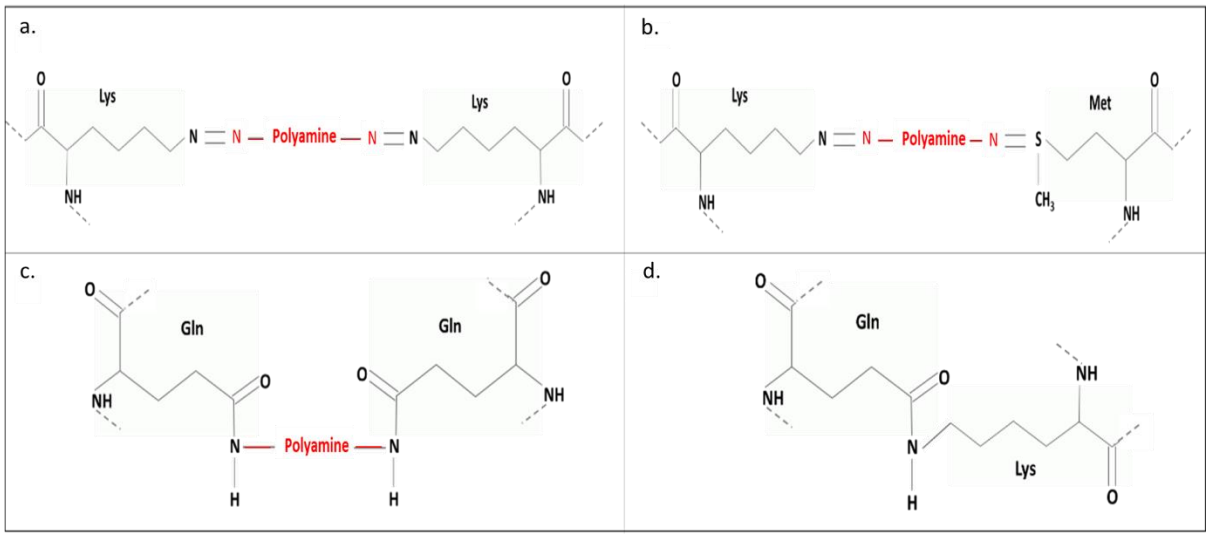

Figure 12. Structure of the possible cross-links. *(a) Bis-ε-lysyl polyamine and (b) ε-lysyl-S-methionyl polyamine cross-links formed by chlorinated polyamine incorporation. (c) Bis-γ-glutamyl polyamine cross-links and (d) ε-(γ-glutamyl)-lysine cross-links formed in TGase catalyzed reaction. Red color indicate the polyamine.*

We could detect bis-ε-lysyl polyamine and ε-lysyl-S-methionyl polyamine cross-links formed by chlorinated polyamine incorporation. In addition, we could find bis-γ-glutamyl polyamine as well as ε-(γ-glutamyl)-lysine cross-links typically catalyzed by transglutaminases (Supplementary figure 1, Supplementary table 1). The number of incorporated chlorinated SPM and SPD did not change significantly while the PUT incorporation increased in $BPNH_2$ treated samples. In SPM treated samples the number of polyamine-chloramine incorporation increased. A similar tendency was observed in the number of transglutaminase catalyzed bis-γ-glutamyl polyamine and ε-(γ-glutamyl)-lysine cross-links (Table 5).

	Bis-ε-lysyl SPM/SPD/PUT			**ε-lysyl-S-methionyl SPM/SPD/PUT**			**Bis-γ-glutamyl SPM/SPD/PUT**			**ε-(γ-glutamyl)-lysine**
NET	**12**	**12**	**12**	**7**	**1**	**1**	**6**	**1**	**1**	**20**
$BPNH_2$	**7**	**11**	**17**	**1**	**2**	**9**	**1**	**4**	**5**	**19**
SPM	**9**	**15**	**19**	**3**	**4**	**6**	**4**	**2**	**5**	**21**

Table 5. Number of protein cross-links between the identified NET proteins. *The values refer to the number of cross-links resulted from three independent StavroX analyzes. Each column refers to the cross-links formed when SPM, SPD, PUT, respectively was present in the crosslink.*

These data indicate the presence of both chloramine-mediated and TGase-mediated cross-links. The network of cross-linked proteins was drawn manually using the results of StavroX analysis

and alterations as a result of the administration of $BPNH_2$ and SPM treatments were observed (Figure 13).

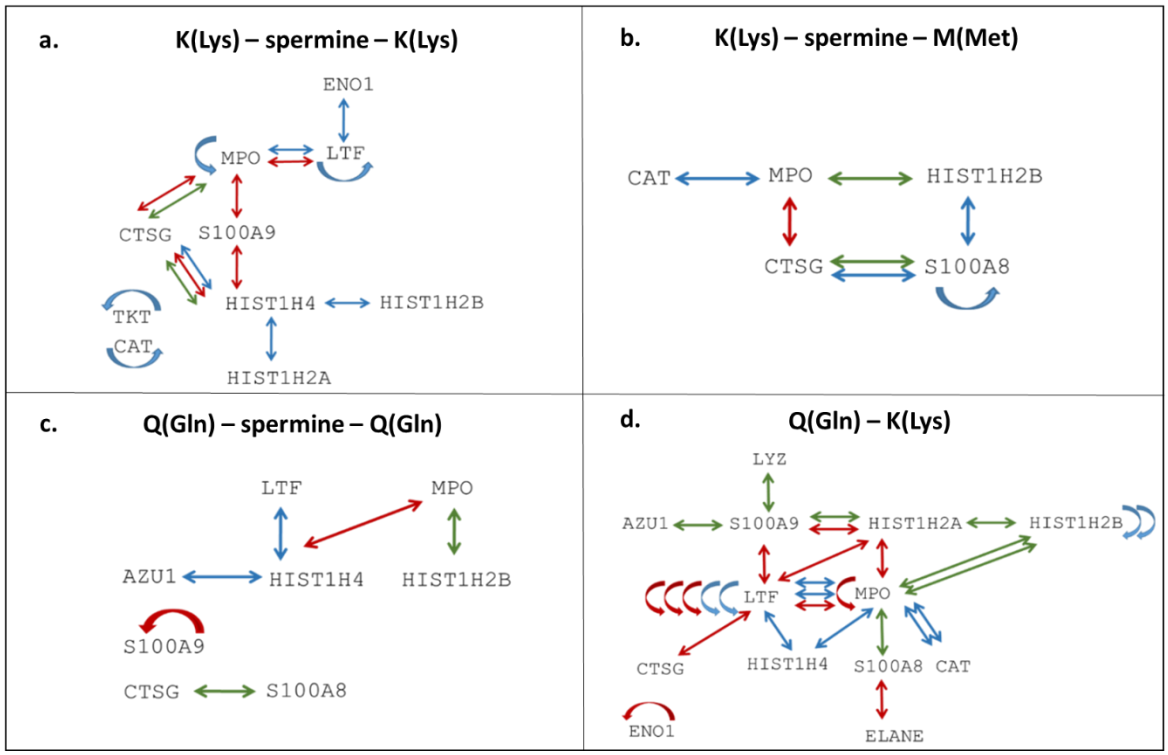

Figure 13. Representative network of cross-linked NET proteins obtained from donor 3. *(a) Bis-ε-lysyl SPM and (b) ε-lysyl-S-methionyl SPM cross-links formed by chlorinated SPM incorporation. (c) Bis-γ-glutamyl SPM cross-links and (d) ε-(γ-glutamyl)-lysine cross-links formed in TGase catalyzed reaction. Blue arrows present NET protein cross-links in Ctrl samples; red arrows indicate cross-links among NET proteins upon $BPNH_2$ treatment, while the green arrows show the protein cross-links formed upon SPM treatment. Curved arrows indicate cross-links between copies of the same protein. In case of the presented cross-linked proteins the Uniprot gene names are used.*

6. Discussion

TGases are enzymes with versatile functions having role in physiological and pathological processes. During my work I examined the role of TGases in PVR and NET formation.

In the first study we could investigate proteins associated with PVR in the vitreous bodies of mice both in the presence and absence of TG2. PVR is a pathological condition arising as a complication of retinal detachment surgery. In spite of the highly increased pathobiological knowledge regarding PVR in the last twenty years, the anatomical and functional results are not sufficient to adequately modify surgical treatments in order to avoid PVR formation. It is likely that surgical methods are no longer able to completely cure or prevent PVR, thus it is important to study the development of PVR and to find possibilities for the modification of the proliferation by drugs [130]. The proliferative process is a normal response of the body leading to scar production. During PVR this process is ineffective and extremely harmful as proliferative membranes are formed on the retinal surface resulting in further retina injury [131]. Many drugs have been tested in cell cultures and animal models that inhibit cell proliferation, epiretinal membrane formation and retina contraction [132,133]. These drugs may have a number of severe side effects and just a few of them can be utilized in clinical treatments. Recently, drug combinations that exert their effects at different stages of the PVR have been tested [133].

It was previously published that the PVR induction upon intravitreal dispase treatment occurs after 14 days following dispase injection in mice [67]. We used this animal model along with two dimensional electrophoresis and mass spectrometry to examine changes related to PVR. The highest changes in protein amounts upon dispase treatment were observed in case of crystallins. They act as chaperones having protective roles and their increased amounts were observed to be related to intensive cell proliferation [126]. The gene expression level of α-, ß- and γ-crystallin was found to be increased after the retinal detachment [134]. Overexpression of alpha-crystallin B was described to have a protective role in retinal epithelial cells against stress-induced apoptosis and secretion of this protein in exosomes has been observed [135,136]. It seems logical that crystallins can be released into the vitreous after retinal injury, which often precedes the PVR formation.

We demonstrated for the first time the increased level of alpha-crystallin B in vitreous upon dispase treatment. The crystallins, especially alpha-crystallin A show an extensive post-translation modification upon dispase treatment, the crystallins identified in the different spots having various pI and size might be due to post-translation modification affecting both the size and the net charge of the protein. It was observed by other groups that the amount of crystallins and their post-

translationally modified forms are altered in oxidative stress following the ischemia-reperfusion injury [137,138], but no experiment was done to elucidate the phenomenon behind the changes affecting crystallins.

Many of differentially expressed proteins in WT PVR mice such as heterogeneous nuclear ribonucleoprotein H, Gln synthetase, ferritin heavy chain, beta-crystallin A1 and grifin were identified in human vitreous proteome [139]. The level of beta-crystallin B2 and S was decreased in WT mice being in consort with human data found in literature showing the presence of beta-crystallin B2 and S in controls but not in patients with PVR [140]. In addition the amount of alpha-crystallin A, beta-crystallin S, tubulin beta and creatine kinase B was reduced in human vitreous proteome of patients with proliferative diabetic retinopathy [141] suggesting the possible implication of these proteins in the proliferative conditions, but we do not known if their decreased level is the cause or the consequence of the proliferative state.

A general strategy to investigate the function of a protein is by knocking out its gene from the genome [142]. In our study we have chosen TG2 to examine its function in PVR. TGase activity is present in the eye and TG2 has been implicated in the development of a variety of ocular diseases such as glaucoma [143], allergic conjunctivitis [144] and cataract [145]. TG2 was located in PVR membranes and it was shown to modulate the phenotype and migration of RPE cells and to control the ECM remodeling in PVR implying its role in the development of PVR [74]. Our hypothesis was that PVR will not form in the lack of TG2, however by OCT examinations the development of PVR was observed in the TG2KO mice.

The alteration of crystallin network was also observed upon dispase treatment. The level of alpha-crystallin A and beta-crystallin B was increased, they have been previously described to inhibit apoptosis and alpha-crystallin, the protein showing the highest changes upon dispase treatment was identified as a substrate for TG2 [146]. It is known that TG2 has an important role during apoptosis. Its absence might be overcome by the overexpression of alpha-crystallins, which most probably have a role in the protection of retinal cells from injury caused by the dispase injection and PVR induction.

Despite the similar pathological outcome at the time point of the analysis a different crystallin profile change was observed in the WT PVR compared to TG2KO PVR. Further study is required to demonstrate whether the TG2 is involved in the timing of the PVR formation. It is not unexpected that the lack of TG2 induces a changed crystallin profile, as TG2 can bind to different substrates depending on the conditions. These data show that more than one type of change in the profile of crystallins might be associated with PVR in mice. It seems that indeed various factors can lead to the crystallin changes observed during dispase injection both in WT and TG2KO mice.

According to the published data and our data, it cannot be assessed if the crystallin profile changes are the cause or the consequence of a proliferative condition in general, and not only of PVR [126]. This means that the solely the examination of the crystallin changes cannot have diagnostic value for PVR.

Considering that dispase is a protease causing limited proteolysis and TG2 is a crosslinking enzyme which generates isopeptide bonds, we can speculate on the possible outcomes of proteolysis in the absence of TG2. It is possible that the lack of protease-resistant cross-link formation leads to an increased crystallin cleavage by dispase. This may be a reason why some spots containing alpha-crystallin are present in the lower MW region of the TG2KO PVR gels.

In conclusion, PVR mice model could be successfully utilized together with 2-DE to analyze the protein changes upon dispase induced PVR formation. The results are in accordance with data reported in the literature. It is interesting to observe that the level of protective crystallins and heat shock protein beta-1 decreases during PVR induction. Further studies are needed to elucidate the molecular basis of this phenomenon. It seems that the lack of TG2 acts as an additional stress factor for the retinal cells and compensatory mechanisms such as the increased level of crystallins seem to come into play. Based on my results I cannot state the exact post-translation modifications of crystallins, but considering the high number of spots containing crystallins, presence of various post-translational modifications can be assumed. It cannot be said how the modifications might affect the function of these proteins, therefore, further functional studies are needed to gain more insight into the function of crystallins and TG2 in the pathogenesis of PVR. In addition, the role of TG2 is predominantly correlated with stabilization of extracellular matrix rather with its functions in apoptosis [147,148]. Inhibition of TG2 via drug treatments or genetic modification can be beneficial for the treatment of TG2-related pathologies and for understanding the molecular details and roles of TG2 in different diseases.

In the second study we have demonstrated that covalent crosslinking of the NET protein as an integral part of functional NET formation can stabilize the components of NET structure. Due to their multiple reactive amino groups it seemed conceivable that polyamines such as SPM, SPD and PUT can lead to intermolecular cross-link formation. Polyamines are known as natural substrates of transglutaminases and transglutaminase-mediated incorporation of polyamines into proteins occurs in cells and tissues [149]. According to the literature, PMA is known to stimulate the neutrophil oxygen metabolism which in the presence of primary amines may result in oxidative amine incorporation into proteins [123]. During the process myeloperoxidase can catalyze the oxidation of chloride to hypochlorous acid in the presence of hydrogen peroxide and both exogenously added amines and endogenous cellular amines can be chlorinated. These chlorinated

amines can react with Lys and Met side chains of the proteins resulting in this way in chloramine incorporation into the proteins [128].

To study NET functionality when polyamine and transglutaminase-dependent cross-linking is prevented we used a monoamine, $BPNH_2$ and a polyamine, SPM which can interfere with the cross-link formation processes. Incorporation of monoamines was detected into cell and NET specific proteins during NETosis as demonstrated by *in situ* immunohistochemistry by colleagues. Different but reproducible $BPNH_2$-labeling patterns were observed comparing cellular proteins to NET specific proteins indicating that protein mono- and polyamination occur in a biochemically-regulated fashion selectively targeting a fraction of the protein in NETosis. Our group could detected the presence of covalently bound monoamines and polyamines on the surface of the NET proteins using specific antibodies to polyamines. In parallel with the exogenous monoamine incorporation significant reduction in the level of the endogenous polyamine incorporation was observed.

Based on the electrophoretic separation on SDS-polyacrylamide gels the pattern of NET proteins originating from different individuals upon various treatments was highly reproducible but the protein composition of the bands was distinct. The fact that the BPNH2 and SPM treatments did not altered significantly the pattern of NET proteins but rather resulted in minor changes in protein composition indicates the robustness of the NET-forming biochemical systems. Many proteins were present in bands not corresponding to their MW suggesting an extensive post-translational processing of proteins during NET formation involving probably both cross-link formation and proteolysis. Eleven proteins identified in band 14 confirms either proteolysis followed by cross-linking of the resulting peptides or cross-linking preceded by proteolytic fragmentation. The investigation of cross-links formed by chlorinated polyamines and transglutaminase-dependent reactions among the proteins indicates the formation of an extensive and specific cross-linking pattern keeping these proteins or their modified and processed forms together.

We could detect the presence of bis-ε-lysyl polyamine and ε-lysyl-S-methionyl polyamine cross-links formed by chlorinated polyamine incorporation and of the TGase catalyzed bis(γ-glutamyl)polyamine and ε-(γ-glutamyl)-lysine cross-links among Lys and Gln at different positions. The number of incorporated chlorinated SPM and SPD did not change significantly while the PUT incorporation increased in BPNH2 treated samples. A similar tendency was observed in the number of transglutaminase catalyzed bis-γ-glutamyl polyamine and ε-(γ-glutamyl)-lysine cross-links. Based on MS/MS data of protein cross-links formed in the $BPNH_2$ and SPM treated NETs we have demonstrated that chlorinated polyamines covalently incorporated into NET proteins and polyamines chlorinated at both of their primary amino groups can form

cross-links between NET proteins contributing to NET stability. We also confirmed that both bis(γ-glutamyl)polyamine and ε-(γ-glutamyl)-lysine cross-links can be formed.

According to the experiments carried out by our collaborators, inhibition of endogenous polyamine incorporation and interference with the cross-linking process leads to impaired pathogen trapping capacity of the NET through the disturbance of its natural structure.

Our results show that endogenous covalent polyamine conjugation and enzymatic cross-linking of NET proteins contribute to the overall stability of NET and are essential for its biological function [136-138].

Based on proteomic data our collaborators investigated the expression and the activity of all types of TGases to ascertain which ones might be responsible for enzymatically mediated conjugation of mono- and polyamines in netosing neutrophils. The gene- and protein expression of TG1 using real-time qPCR and western blot, respectively was detected. The specific TG1 activity was observed in neutrophil cell lysate by ELISA.

In conclusion, our data indicate that the presence of polyamines, MPO and TG1 together is required for the proper NET stabilization.

7. Keywords/kulcsszavak

Transglutaminases, proliferative vitreoretinopathy, neutrophil extracellular trap, 2D gel electrophoresis, mass spectrometry, polyamines, cross-link

Transzglutaminázok, proliferatív vitreoretinopátia, neutrofil extracelluláris csapda, 2D gélelektroforézis, tömegspektrometria, poliaminok, keresztkötés

8. Summary

Transglutaminases (TGases) are widely investigated Ca^{2+}-dependent enzymes with diverse functions. They play a role in numerous essential physiological and pathological processes via catalyzing the isopeptide bond formation between lysine and glutamine residues leading to the formation of ε-(γ-glutamyl)-lysine bonds.

In the first study our aim was to identify proteins associated with proliferative vitreoretinopathy (PVR) in the vitreous bodies of mice using two dimensional electrophoresis and mass spectrometry-based protein identification. We could demonstrate proteins related to PVR in the vitreous bodies of mice both in the presence and lack of TG2. Highest changes in the amount of different forms of crystallins upon dispase treatment were detected. In addition a different crystallin profile change was observed in the wild-type PVR group compared to TG2 knock-out PVR group. The utilization of PVR mice model along with two-dimension gel electrophoresis to analyze the protein changes upon dispase induced PVR formation and the effect of the lack of TG2 was successful. The results are in accordance with data reported in the literature, but further functional studies are needed to elucidate the molecular basis of this phenomenon.

In the second study our aim was to investigate the protein cross-links and how the protein crosslink-profile changes during neutrophil extracellular trap (NET) formation upon $BPNH_2$ and SPM treatments. NET proteins were analyzed by electrophoresis and HPLC-coupled tandem mass spectrometry on a 4000 QTRAP mass spectrometer. Based on MS/MS data, the site and the type of cross-links formed were identified using StavroX protein cross-link examination software. We could demonstrate the changes in the protein cross-linking patterns upon the applied treatments and according to our data for the cross-linked protein network formation two processes are responsible: both the TGase and the myeloperoxidase (MPO)-catalyzed polyamine chloramine mediated crosslinks are important. Our data showed that the presence of MPO and TGases together is required for proper NET stabilization.

9. Összefoglalás

A transzglutaminázok (TGázok) széles körben vizsgált Ca^{2+}-függő enzimek, melyek változatos funkciókkal rendelkeznek. Számos esszenciális fiziológiás és patológiás folyamatban játszanak szerepet azáltal, hogy katalizálják az ε-(γ-glutamil)-lizin izopeptid kötések létrejöttét a lizin és glutamin aminosav oldalláncok között.

Munkám első felében az volt a célom, hogy egerek üvegtesti mintáiban kétdimenziós gélelektroforézis és tömegspektrometria alapú fehérje azonosítás alkalmazásával olyan fehérjéket azonosítsak, amelyek összefüggésben állnak a proliferatív vitreoretinopátiával (PVR). TG2 jelenlétében és hiányában egyaránt sikerült kimutatnom a PVR-hez köthető fehérjéket az egér üvegtesti mintákban. A diszpáz kezelés hatására a krisztallinok különböző formáinak mennyiségében figyeltem meg a legjelentősebb változásokat, mindemellett eltérő krisztallin profil változást tapasztaltam a vad típusú PVR és TG2 knock-out PVR csoportokban. Munkám során sikerrel alkalmaztam a kétdimenziós elektroforézist és a PVR egérmodellt a diszpáz által indukált PVR-re jellemző fehérje változások és a TG2 hiányában bekövetkező változások tanulmányozására. Eredményeim jó egyezést mutatnak az irodalmi adatokkal, de további funkcionális vizsgálatok szükségesek a megfigyelt jelenség mögött húzódó molekuláris magyarázat felderítésére.

Munkám második felében az volt a célom, hogy megvizsgáljam a fehérje keresztkötéseket, illetve azt, hogy hogyan változik a fehérje keresztkötés-profil a neutrofil extracelluláris csapda (NET) képződés során 5-(biotinamido)-pentil-amin és spermin kezelések hatására. A NET fehérjéket elektroforézis és folyadék kromatográffal-kapcsolt tandem tömegspektrometriával tanulmányoztam 4000 QTRAP tömegspektrométeren. Az MS/MS adatok alapján a keletkezett keresztkötések helyét és típusát StavroX keresztkötött fehérje vizsgáló szoftver segítségével azonosítottam. A fehérje keresztkötés mintázatokban változásokat mutattam ki a kezelések hatására. Adataim alapján megállapítható, hogy a keresztkötött fehérje hálózat kialakításáért két folyamat felelős: a TGázok és az mieloperoxidáz (MPO) által katalizált folyamatok, amelyek poliamin klóraminok keresztkötését hozzák létre. Adataink azt mutatták, hogy az MPO és a TGázok együttes jelenléte szükséges a NET megfelelő stabilizációjához.

10. Acknowledgement

Among all those who contributed to this PhD thesis, first of all I would like to express my gratitude to my supervisor Dr. Éva Csősz for the continuous support, for the scientific discussions and for the opportunities she offered me during my studies.

I am grateful to Prof. László Fésüs and Prof. József Tőzsér, the former and recent heads of the Department of Biochemistry and Molecular Biology for the opportunity to work in a well-equipped environment.

I acknowledge the collaboration with the research group of Prof. László Fésüs, especially the help of Dr. Endre Károly Kristóf who helped me during neutrophil isolation and infection.

I would like to thank Prof. Goran Petrovski for providing us the mice vitreous bodies for protein profile analyses.

I am thankful for the help of my former and recent colleagues in the Proteomics Core Facility especially my dear friends Dr. Gergő Kalló, Péter Lábiscsák, Eszter Deák, Beáta Sipos, Kamilla Sólyom, Tímea Székely, Dr. Krisztina Joóné Matúz and Zsuzsanna Pató.

I would like to thank the help of the members of the Laboratory of Retroviral Biochemistry.

Last but not least I wish to express my greatest gratitude to my husband and my family for their help, support and encouragement in any situation of my life.

11. References

1. Folk JE, Finlayson JS. The epsilon-(gamma-glutamyl)lysine crosslink and the catalytic role of transglutaminases. Adv Protein Chem. 1977;31: 1–133.

2. Fesus L, Piacentini M. Transglutaminase 2: an enigmatic enzyme with diverse functions. Trends Biochem Sci. 2002;27: 534–9.

3. Lorand L, Graham RM. Transglutaminases: crosslinking enzymes with pleiotropic functions. Nat Rev Mol Cell Biol. 2003;4: 140–156. doi:10.1038/nrm1014

4. Murthy SNP, Iismaa S, Begg G, Freymann DM, Graham RM, Lorand L. Conserved tryptophan in the core domain of transglutaminase is essential for catalytic activity. Proc Natl Acad Sci U S A. 2002;99: 2738–42. doi:10.1073/pnas.052715799

5. Kieliszek M, Misiewicz A. Microbial transglutaminase and its application in the food industry. A review. Folia Microbiol (Praha). 2014;59: 241–50. doi:10.1007/s12223-013-0287-x

6. Della Mea M, Caparrós-Ruiz D, Claparols I, Serafini-Fracassini D, Rigau J. AtPng1p. The First Plant Transglutaminase. PLANT Physiol. 2004;135: 2046–2054. doi:10.1104/pp.104.042549

7. Nozawa H, Mamegoshi S, Seki N. Partial Purification and Characterization of Six Transglutaminases from Ordinary Muscles of Various Fishes and Marine Invertebrates. Comp Biochem Physiol Part B Biochem Mol Biol. 1997;118: 313–317. doi:10.1016/S0305-0491(97)00062-X

8. Yoshiyuki K, Koh-Ichiro S, Katsuya S, Hisashi Y, Noriki N A, M M. Purification and Characterization of Transglutaminase from Japanese Oyster (Crassostrea gigas). J Agric Food Chem. American Chemical Society; 1997; 604–610. doi:10.1021/JF9604596

9. Beninati S, Piacentini M. The transglutaminase family: an overview: Minireview article. Amino Acids. 2004;26. doi:10.1007/s00726-004-0091-7

10. Esposito C, Caputo I. Mammalian transglutaminases.Identification of substrates as a key to physiological function and physiopathological relevance. FEBS J. Blackwell Science Ltd; 2005;272: 615–631. doi:10.1111/j.1742-4658.2004.04476.x

11. Griffin M, Casadio R, Bergamini CM. Transglutaminases: Nature's biological glues. Biochem J. 2002;368: 377–96. doi:10.1042/BJ20021234

12. Inbal A, Lubetsky A, Krapp T, Castel D, Shaish A, Dickneitte G, et al. Impaired wound healing in factor XIII deficient mice. Thromb Haemost. 2005;94: 432–7. doi:10.1160/TH05-04-0291

13. Birben E, Oner R, Oner C, Gumruk F, Altay C, Gurgey A. Mutations in coagulation factor XIII A gene in three Turkish patients: two novel mutations and a known insertion. Br J Haematol. 2002;118: 278–281. doi:10.1046/j.1365-2141.2002.03571.x

14. Heinle K, Adam O, Rauh G. Factor XIII insufficiency in a patient with severe psoriasis vulgaris, arthritis, and infirmity. Clin Rheumatol. 1998;17: 346–8.

15. Schubring C, Grulich-Henn J, Burkhard P, Klöss HR, Selmayr E, Müller-Berghaus G. Fibrinolysis and factor XIII in women with spontaneous abortion. Eur J Obstet Gynecol Reprod Biol. 1990;35: 215–21.

16. Candi E, Melino G, Lahm A, Ceci R, Rossi A, Kim IG, et al. Transglutaminase 1 mutations in lamellar ichthyosis. Loss of activity due to failure of activation by proteolytic processing. J Biol Chem. 1998;273: 13693–702.

17. Nurminskaya M, Belkin A. Cellular functions of tissue transglutaminase. Int Rev Cell Mol Biol. 2012;294: 1–97. doi:10.1016/B978-0-12-394305-7.00001-X

18. Kuo T-F, Tatsukawa H, Kojima S. New insights into the functions and localization of nuclear transglutaminase 2. FEBS J. 2011;278: 4756–4767. doi:10.1111/j.1742-4658.2011.08409.x

19. Facchiano F, Facchiano A, Facchiano AM. The role of transglutaminase-2 and its substrates in human diseases. Front Biosci. 2006;11: 1758–73.

20. Eckert RL, Kaartinen MT, Nurminskaya M, Belkin AM, Colak G, Johnson GVW, et al. Transglutaminase regulation of cell function. Physiol Rev. 2014;94: 383–417. doi:10.1152/physrev.00019.2013

21. Preisz K, Sardy M, Horvath A, Karpati S. Immunoglobulin, complement and epidermal transglutaminase deposition in the cutaneous vessels in dermatitis herpetiformis. J Eur Acad Dermatology Venereol. 2005;19: 74–79. doi:10.1111/j.1468-3083.2004.01132.x

22. Iismaa SE. The prostate-specific protein, transglutaminase 4 (TG4), is an autoantigen associated with male subfertility. Ann Transl Med. AME Publications; 2016;4: S35. doi:10.21037/atm.2016.10.02

23. Jiang WG, Ablin RJ. Prostate transglutaminase: a unique transglutaminase and its role in prostate cancer. Biomark Med. 2011;5: 285–291. doi:10.2217/bmm.11.36

24. Candi E, Oddi S, Paradisi A, Terrinoni A, Ranalli M, Teofoli P, et al. Expression of Transglutaminase 5 in Normal and Pathologic Human Epidermis. J Invest Dermatol. 2002;119: 670–677. doi:10.1046/j.1523-1747.2002.01853.x

25. Thomas H, Beck K, Adamczyk M, Aeschlimann P, Langley M, Oita RC, et al. Transglutaminase 6: a protein associated with central nervous system development and motor function. Amino Acids. 2013;44: 161–77. doi:10.1007/s00726-011-1091-z

26. Odii BO, Coussons P. Biological functionalities of transglutaminase 2 and the possibility of its compensation by other members of the transglutaminase family. Sci World J. Hindawi; 2014;2014: 714561. doi:10.1155/2014/714561

27. Guan W, Xia K, Ma Y, Liu Y, Shi Y, Jiang H, et al. Transglutaminase 6 interacts with polyQ proteins and promotes the formation of polyQ aggregates. Biochem Biophys Res Commun. 2013;437: 94–100. doi:10.1016/j.bbrc.2013.06.044

28. Wang JL, Yang X, Xia K, Hu ZM, Weng L, Jin X, et al. TGM6 identified as a novel causative gene of spinocerebellar ataxias using exome sequencing. Brain. 2010;133: 3510–3518. doi:10.1093/brain/awq323

29. Jiang WG, Ablin R, Douglas-Jones A, Mansel RE. Expression of transglutaminases in human breast cancer and their possible clinical significance. Oncol Rep. 2003;10: 2039–44.

30. Jarolim P, Palek J, Rubin H, Prchal J, Korsgren C, Cohen C. Band 3 Tuscaloosa: Pro327-Arg327 substitution in the cytoplasmic domain of erythrocyte band 3 protein associated with spherocytic hemolytic anemia and partial deficiency of protein 4.2. Blood. 1992;80(2):523-: 523–9.

31. Facchiano A, Facchiano F. Transglutaminases and their substrates in biology and human diseases: 50 years of growing. Amino Acids. 2009;36: 599–614. doi:10.1007/s00726-008-0124-8

32. Csősz É, Meskó B, Fésüs L. Transdab wiki: the interactive transglutaminase substrate database on web 2.0 surface. Amino Acids. 2009;36: 615–617. doi:10.1007/s00726-008-0121-y

33. Beninati S, Martinet N, Folk JE. High-performance liquid chromatographic method for the

determination of epsilon-(gamma-glutamyl)lysine and mono- and bis-gamma-glutamyl derivatives of putrescine and spermidine. J Chromatogr. 1988;443: 329–35.

34. Eckert RL, Wzy A, Sturniolo MT, Broome A-M, Ruse M, Rorkez EA. Transglutaminase Function in Epidermis. J Invest Dermatol. 2005;124: 481–492. doi:10.1111/j.0022-202X.2005.23627.x

35. Kalinin AE, Kajava A V., Steinert PM. Epithelial barrier function: assembly and structural features of the cornified cell envelope. BioEssays. 2002;24: 789–800. doi:10.1002/bies.10144

36. Hennings H, Steinert P, Buxman MM. Calcium induction of transglutaminase and the formation of epsilon(gamma-glutamyl) lysine cross-links in cultured mouse epidermal cells. Biochem Biophys Res Commun. 1981;102: 739–45.

37. Saunders NA, Bernacki SH, Vollberg TM, Jetten AM. Regulation of transglutaminase type I expression in squamous differentiating rabbit tracheal epithelial cells and human epidermal keratinocytes: effects of retinoic acid and phorbol esters. Mol Endocrinol. 1993;7: 387–398. doi:10.1210/mend.7.3.8097865

38. Thangaraju K, Biri B, Schlosser G, Kiss B, Nyitray L, Fésüs L, et al. Real-time kinetic method to monitor isopeptidase activity of transglutaminase 2 on protein substrate. Anal Biochem. 2016;505: 36–42. doi:10.1016/j.ab.2016.04.012

39. Mishra S, Melino G, Murphy LJ. Transglutaminase 2 Kinase Activity Facilitates Protein Kinase A-induced Phosphorylation of Retinoblastoma Protein. J Biol Chem. 2007;282: 18108–18115. doi:10.1074/jbc.M607413200

40. Nakaoka H, Perez DM, Baek KJ, Das T, Husain A, Misono K, et al. Gh: a GTP-binding protein with transglutaminase activity and receptor signaling function. Science. 1994;264: 1593–6.

41. Im MJ, Russell MA, Feng JF. Transglutaminase II: a new class of GTP-binding protein with new biological functions. Cell Signal. 1997;9: 477–82.

42. Hasegawa G, Suwa M, Ichikawa Y, Ohtsuka T, Kumagai S, Kikuchi M, et al. A novel function of tissue-type transglutaminase: protein disulphide isomerase. Biochem J. 2003;373: 793–803. doi:10.1042/BJ20021084

43. Odii BO, Coussons P. Biological functionalities of transglutaminase 2 and the possibility of its compensation by other members of the transglutaminase family. Sci World J. 2014;2014: 714561. doi:10.1155/2014/714561

44. Matsuki M, Yamashita F, Ishida-Yamamoto A, Yamada K, Kinoshita C, Fushiki S, et al. Defective stratum corneum and early neonatal death in mice lacking the gene for transglutaminase 1 (keratinocyte transglutaminase). Proc Natl Acad Sci U S A. 1998;95: 1044–9.

45. Arentz-Hansen H, Körner R, Molberg O, Quarsten H, Vader W, Kooy YM, et al. The intestinal T cell response to alpha-gliadin in adult celiac disease is focused on a single deamidated glutamine targeted by tissue transglutaminase. J Exp Med. 2000;191: 603–12.

46. Olsen KC, Sapinoro RE, Kottmann RM, Kulkarni AA, Iismaa SE, Johnson GVW, et al. Transglutaminase 2 and its role in pulmonary fibrosis. Am J Respir Crit Care Med. 2011;184: 699–707. doi:10.1164/rccm.201101-0013OC

47. Verderio E, Johnson T, Griffin M. Tissue transglutaminase in normal and abnormal wound healing: review article. Amino Acids. 2004;26: 387–404. doi:10.1007/s00726-004-0094-4

48. Tatsukawa H, Furutani Y, Hitomi K, Kojima S. Transglutaminase 2 has opposing roles in the regulation of cellular functions as well as cell growth and death. Cell Death Dis. 2016;7: e2244. doi:10.1038/cddis.2016.150

49. Williams H, Pease RJ, Newell LM, Cordell PA, Graham RM, Kearney MT, et al. Effect of transglutaminase 2 (TG2) deficiency on atherosclerotic plaque stability in the apolipoprotein E deficient mouse. Atherosclerosis. 2010;210: 94–9. doi:10.1016/j.atherosclerosis.2009.11.014

50. Ruan Q, Johnson GVW. Transglutaminase 2 in neurodegenerative disorders. Front Biosci. 2007;12: 891–904.

51. Hwang JY, Mangala LS, Fok JY, Lin YG, Merritt WM, Spannuth WA, et al. Clinical and Biological Significance of Tissue Transglutaminase in Ovarian Carcinoma. Cancer Res. 2008;68: 5849–5858. doi:10.1158/0008-5472.CAN-07-6130

52. Chihong Z, Yutian L, Danying W, Ruibin J, Huaying S, Linhui G, et al. Prognostic value of Transglutaminase 2 in non-small cell lung cancer patients. Oncotarget. 2017;8: 45577–45584. doi:10.18632/oncotarget.17374

53. Verma A, Wang H, Manavathi B, Fok JY, Mann AP, Kumar R, et al. Increased Expression of Tissue Transglutaminase in Pancreatic Ductal Adenocarcinoma and Its Implications in Drug Resistance and Metastasis. Cancer Res. 2006;66: 10525–10533. doi:10.1158/0008-

5472.CAN-06-2387

54. Yuan L, Holmes TC, Watts RE, Khosla C, Broekelmann TJ, Mecham R, et al. Novel chemo-sensitizing agent, ERW1227B, impairs cellular motility and enhances cell death in glioblastomas. J Neurooncol. 2011;103: 207–219. doi:10.1007/s11060-010-0379-2

55. Gundemir S, Monteagudo A, Akbar A, Keillor JW, Johnson GVW. The complex role of transglutaminase 2 in glioblastoma proliferation. Neuro Oncol. 2016;6: now157. doi:10.1093/neuonc/now157

56. Fok JY, Ekmekcioglu S, Mehta K. Implications of tissue transglutaminase expression in malignant melanoma. Mol Cancer Ther. 2006;5: 1493–1503. doi:10.1158/1535-7163.MCT-06-0083

57. Salter NW, Ande SR, Nguyen HK, Nyomba BLG, Mishra S. Functional characterization of naturally occurring transglutaminase 2 mutants implicated in early-onset type 2 diabetes. J Mol Endocrinol. 2012;48: 203–216. doi:10.1530/JME-11-0064

58. De Laurenzi V, Melino G. Gene Disruption of Tissue Transglutaminase. Mol Cell Biol. 2001;21: 148–155. doi:10.1128/MCB.21.1.148-155.2001

59. Tong L, Png E, Aihua H, Yong SS, Yeo HL, Riau A, et al. Molecular mechanism of transglutaminase-2 in corneal epithelial migration and adhesion. Biochim Biophys Acta. 2013;1833: 1304–15. doi:10.1016/j.bbamcr.2013.02.030

60. Nanda N, Iismaa SE, Owens WA, Husain A, Mackay F, Graham RM. Targeted Inactivation of G h /Tissue Transglutaminase II. J Biol Chem. 2001;276: 20673–20678. doi:10.1074/jbc.M010846200

61. Falasca L, Iadevaia V, Ciccosanti F, Melino G, Serafino A, Piacentini M. Transglutaminase type II is a key element in the regulation of the anti-inflammatory response elicited by apoptotic cell engulfment. J Immunol. 2005;174: 7330–40.

62. Pastor JC. Proliferative vitreoretinopathy: an overview. Surv Ophthalmol. 1988;43: 3–18.

63. Pastor J, de la Rúa E, Martín F. Proliferative vitreoretinopathy: Risk factors and pathobiology. Prog Retin Eye Res. 2002;21: 127–144. doi:10.1016/S1350-9462(01)00023-4

64. Hiscott P, Sheridan C, Magee RM, Grierson I. Matrix and the retinal pigment epithelium in proliferative retinal disease. Prog Retin Eye Res. 1999;18: 167–190. doi:10.1016/S1350-

9462(98)00024-X

65. Yang S, Li H, Li M, Wang F. Mechanisms of epithelial-mesenchymal transition in proliferative vitreoretinopathy. Discov Med. 2015;20: 207–17.

66. Campochiaro PA, Jerdan JA, Glaser BM, Cardin A, Michels RG. Vitreous aspirates from patients with proliferative vitreoretinopathy stimulate retinal pigment epithelial cell migration. Arch Ophthalmol. 1985;103: 1403–5.

67. Johnsen EO, Froen RC, Albert R, Omdal BK, Sarang Z, Berta A, et al. Activation of neural progenitor cells in human eyes with proliferative vitreoretinopathy. Exp Eye Res. 2012;98: 28–36. doi:10.1016/j.exer.2012.03.008

68. Bastiaans J, van Meurs JC, Mulder VC, Nagtzaam NMA, Smits-te Nijenhuis M, Dufour-van den Goorbergh DC, et al. The role of thrombin in proliferative vitreoretinopathy. Invest Ophthalmol Vis Sci. 2014;55: 4659–66. doi:10.1167/iovs.14-14818

69. Yu J, Liu F, Cui S-J, Liu Y, Song Z-Y, Cao H, et al. Vitreous proteomic analysis of proliferative vitreoretinopathy. Proteomics. 2008;8: 3667–78. doi:10.1002/pmic.200700824

70. Kon CH, Occleston NL, Charteris D, Daniels J, Aylward GW, Khaw PT. A prospective study of matrix metalloproteinases in proliferative vitreoretinopathy. Invest Ophthalmol Vis Sci. 1998;39: 1524–9.

71. Gandorfer A. Enzymatic vitreous disruption. Eye. 2008;22: 1273–7. doi:10.1038/eye.2008.29

72. Velazquez OC. Angiogenesis and vasculogenesis: inducing the growth of new blood vessels and wound healing by stimulation of bone marrow-derived progenitor cell mobilization and homing. J Vasc Surg. 2007;45: 39–47. doi:10.1016/j.jvs.2007.02.068

73. Haroon ZA, Hettasch JM, Lai TS, Dewhirst MW, Greenberg CS. Tissue transglutaminase is expressed, active, and directly involved in rat dermal wound healing and angiogenesis. FASEB J. 1999;13: 1787–95.

74. Priglinger SG, May C a., Neubauer AS, Alge CS, Schönfeld CL, Kampik A, et al. Tissue transglutaminase as a modifying enzyme of the extracellular matrix in PVR membranes. Investig Ophthalmol Vis Sci. 2003;44: 355–364. doi:10.1167/iovs.02-0224

75. Kobayashi SD, DeLeo FR. Role of neutrophils in innate immunity: a systems biology-level approach. Wiley Interdiscip Rev Syst Biol Med. 2009;1: 309–33. doi:10.1002/wsbm.32

76. Urban CF, Lourido S, Zychlinsky A. How do microbes evade neutrophil killing? Cell Microbiol. 2006;8: 1687–1696. doi:10.1111/j.1462-5822.2006.00792.x

77. Guimaraes-Costa AB, Nascimento MTC, Wardini AB, Pinto-da-Silva LH, Saraiva EM. ETosis: A Microbicidal Mechanism beyond Cell Death. J Parasitol Res. 2012;2012: 1–11. doi:10.1155/2012/929743

78. Hirsch JG. Bactericidal action of histone. J Exp Med. 1958;108: 925–44.

79. Segal AW. How neutrophils kill microbes. Annu Rev Immunol. 2005;23: 197–223. doi:10.1146/annurev.immunol.23.021704.115653

80. Brinkmann V, Zychlinsky A. Neutrophil extracellular traps: is immunity the second function of chromatin? J Cell Biol. 2012;198: 773–83. doi:10.1083/jcb.201203170

81. Zawrotniak M, Rapala-Kozik M. Neutrophil extracellular traps (NETs) - Formation and implications. Acta Biochim Pol. 2013;60: 277–284.

82. Lu T, Kobayashi SD, Quinn MT, Deleo FR. A NET Outcome. Front Immunol. 2012;3: 365. doi:10.3389/fimmu.2012.00365

83. Papayannopoulos V, Metzler KD, Hakkim A, Zychlinsky A. Neutrophil elastase and myeloperoxidase regulate the formation of neutrophil extracellular traps. J Cell Biol. 2010;191: 677–91. doi:10.1083/jcb.201006052

84. Belaaouaj A, McCarthy R, Baumann M, Gao Z, Ley TJ, Abraham SN, et al. Mice lacking neutrophil elastase reveal impaired host defense against gram negative bacterial sepsis. Nat Med. 1998;4: 615–618. doi:10.1038/nm0598-615

85. Tkalcevic J, Novelli M, Phylactides M, Iredale JP, Segal AW, Roes J. Impaired immunity and enhanced resistance to endotoxin in the absence of neutrophil elastase and cathepsin G. Immunity. 2000;12: 201–10.

86. Metzler KD, Fuchs TA, Nauseef WM, Reumaux D, Roesler J, Schulze I, et al. Myeloperoxidase is required for neutrophil extracellular trap formation: implications for innate immunity. Blood. 2011;117: 953–9. doi:10.1182/blood-2010-06-290171

87. Karlsson A, Nixon JB, McPhail LC. Phorbol myristate acetate induces neutrophil NADPH-oxidase activity by two separate signal transduction pathways: dependent or independent of phosphatidylinositol 3-kinase. J Leukoc Biol. 2000;67: 396–404.

88. Parker H, Dragunow M, Hampton MB, Kettle AJ, Winterbourn CC. Requirements for NADPH oxidase and myeloperoxidase in neutrophil extracellular trap formation differ depending on the stimulus. J Leukoc Biol. 2012;92: 841–9. doi:10.1189/jlb.1211601

89. Legrain P, Aebersold R, Archakov A, Bairoch A, Bala K, Beretta L, et al. The human proteome project: current state and future direction. Mol Cell Proteomics. 2011;10. doi:10.1074/mcp.M111.009993

90. Hood LE, Omenn GS, Moritz RL, Aebersold R, Yamamoto KR, Amos M, et al. New and improved proteomics technologies for understanding complex biological systems: addressing a grand challenge in the life sciences. Proteomics. 2012;12: 2773–83. doi:10.1002/pmic.201270086

91. Zhang Y, Fonslow BR, Shan B, Baek M-C, Yates JR. Protein Analysis by Shotgun/Bottom-up Proteomics. Chem Rev. 2013;113: 2343–2394. doi:10.1021/cr3003533

92. Resing KA, Ahn NG. Proteomics strategies for protein identification. FEBS Lett. 2005;579: 885–889. doi:10.1016/J.FEBSLET.2004.12.001

93. Lindemann C, Thomanek N, Hundt F, Lerari T, Meyer HE, Wolters D, et al. Strategies in relative and absolute quantitative mass spectrometry based proteomics. Biol Chem. 2017;398: 687–699. doi:10.1515/hsz-2017-0104

94. Zhao Y, Jensen ON. Modification-specific proteomics: strategies for characterization of post-translational modifications using enrichment techniques. Proteomics. 2009;9: 4632–41. doi:10.1002/pmic.200900398

95. Maheshwari S, Brylinski M. Across-proteome modeling of dimer structures for the bottom-up assembly of protein-protein interaction networks. BMC Bioinformatics. 2017;18: 257. doi:10.1186/S12859-017-1675-Z

96. Siuti N, Kelleher NL. Decoding protein modifications using top-down mass spectrometry. Nat Methods. 2007;4: 817–821. doi:10.1038/nmeth1097

97. Tran JC, Zamdborg L, Ahlf DR, Lee JE, Catherman AD, Durbin KR, et al. Mapping intact protein isoforms in discovery mode using top-down proteomics. Nature. 2011;480: 254–8. doi:10.1038/nature10575

98. Rabilloud T, Chevallet M, Luche S, Lelong C. Two-dimensional gel electrophoresis in proteomics: Past, present and future. J Proteomics. 2010;73: 2064–77.

doi:10.1016/j.jprot.2010.05.016

99. Rabilloud T, Lelong C. Two-dimensional gel electrophoresis in proteomics: A tutorial. J Proteomics. 2011;74: 1829–1841. doi:10.1016/J.JPROT.2011.05.040

100. Berth M, Moser FM, Kolbe M, Bernhardt J. The state of the art in the analysis of two-dimensional gel electrophoresis images. Appl Microbiol Biotechnol. 2007;76: 1223–1243. doi:10.1007/s00253-007-1128-0

101. Gygi SP, Corthals GL, Zhang Y, Rochon Y, Aebersold R. Evaluation of two-dimensional gel electrophoresis-based proteome analysis technology. Proc Natl Acad Sci U S A. 2000;97(17): 9390–5.

102. López JL. Two-dimensional electrophoresis in proteome expression analysis. J Chromatogr B. 2007;849: 190–202. doi:10.1016/j.jchromb.2006.11.049

103. Liu S, Zhang Y, Xie X, Hu W, Cai R, Kang J, et al. Application of two-dimensional electrophoresis in the research of retinal proteins of diabetic rat. Cell Mol Immunol. 2007;4: 65–70.

104. Murphy S, Dowling P, Ohlendieck K. Comparative Skeletal Muscle Proteomics Using Two-Dimensional Gel Electrophoresis. Proteomes. 2016;4: 27. doi:10.3390/proteomes4030027

105. Alfonso P, Núnez A, Madoz-Gurpide J, Lombardia L, Sánchez L, Casal JI. Proteomic expression analysis of colorectal cancer by two-dimensional differential gel electrophoresis. Proteomics. 2005;5: 2602–2611. doi:10.1002/pmic.200401196

106. Gulyás G, Czeglédi L, Béri B, Harangi S, Csősz E, Szabó Z, et al. Proteomic analysis of skeletal muscle at different live weights in Charolais bulls. Acta Aliment. 2015;44: 132–138. doi:10.1556/AAlim.44.2015.1.14

107. Márkus B, Szabó K, Pfliegler WP, Petrényi K, Boros E, Pócsi I, et al. Proteomic analysis of protein phosphatase Z1 from Candida albicans. PLoS One. 2017;12. doi:10.1371/journal.pone.0183176

108. Gharbi S, Gaffney P, Yang A, Zvelebil MJ, Cramer R, Waterfield MD, et al. Evaluation of Two-dimensional Differential Gel Electrophoresis for Proteomic Expression Analysis of a Model Breast Cancer Cell System. Mol Cell Proteomics. 2002;1: 91–98. doi:10.1074/mcp.T100007-MCP200

109. Li H, Su J, Chiu C, Lin J, Yang Z, Hwang W, et al. Proteomic Investigation of the Sinulariolide-Treated Melanoma Cells A375: Effects on the Cell Apoptosis through Mitochondrial-Related Pathway and Activation of Caspase Cascade. Mar Drugs. 2013;11: 2625–2642. doi:10.3390/md11072625

110. Cottrell JS. Protein identification using MS/MS data. J Proteomics. 2011;74: 1842–1851. doi:10.1016/j.jprot.2011.05.014

111. Canas B, López-Ferrer D, Ramos-Fernández A, Camafeita E, Calvo E. Mass spectrometry technologies for proteomics. Briefings Funct Genomics Proteomics. 2006;4: 295–320. doi:10.1093/bfgp/eli002

112. Volmer LSDA. Tutorial - Mass Analyzers: An Overview of Several Designs and Their Applications, Part II. Spectroscopy. 2005;20.

113. Tuli L, Ressom HW. LC-MS Based Detection of Differential Protein Expression. J Proteomics Bioinform. 2009;2: 416–438. doi:10.4172/jpb.1000102

114. Kaneko N, Yamamoto R, Sato T, Tanaka K. Identification and quantification of amyloid beta-related peptides in human plasma using matrix-assisted laser desorption/ionization time-of-flight mass spectrometry. Proc Jpn Acad Ser B Phys Biol Sci. 2014;90: 104–17.

115. Fenn BJ. Electrospray ionization mass spectrometry: How it all began. J ournal Biomol Tech. 2002; doi:13(3):101-18

116. Aebersold R, Goodlett DR. Mass Spectrometry in Proteomics. Chem Rev. 2001;101: 269–296. doi:10.1021/cr990076h

117. Aebersold R, Mann M. Mass spectrometry-based proteomics. Nature. 2003;422: 198–207. doi:10.1038/nature01511

118. Cantó Soler MV, Gallo JE, Dodds R, Suburo AM. A mouse model of proliferative vitreoretinopathy induced by dispase. Exp Eye Res. 2002;75: 491–504. doi:10.1006/exer.2002.2031

119. Rabilloud T, Strub JM, Luche S, van Dorsselaer A, Lunardi J. A comparison between Sypro Ruby and ruthenium II tris (bathophenanthroline disulfonate) as fluorescent stains for protein detection in gels. Proteomics. 2001;1: 699–704. doi:10.1002/1615-9861(200104)1:5<699::AID-PROT699>3.0.CO;2-C

120. Martin D, Brun C, Remy E, Mouren P, Thieffry D, Jacq B. GOToolBox: functional analysis of gene datasets based on Gene Ontology. Genome Biol. 2004;5: R101. doi:10.1186/gb-2004-5-12-r101

121. Szklarczyk D, Franceschini A, Wyder S, Forslund K, Heller D, Huerta-Cepas J, et al. STRING v10: protein-protein interaction networks, integrated over the tree of life. Nucleic Acids Res. 2015;43: D447–D452. doi:10.1093/nar/gku1003

122. Nauseef WM. Isolation of Human Neutrophils from Venous Blood. Methods in molecular biology (Clifton, NJ). 2014. pp. 13–18. doi:10.1007/978-1-62703-845-4_2

123. Thomas EL, Jefferson MM, Grisham MB. Myeloperoxidase-catalyzed incorporation of amines into proteins: role of hypochlorous acid and dichloramines. Biochemistry. 1982;21: 6299–308.

124. Bradford MM. A rapid and sensitive method for the quantitation of microgram quantities of protein utilizing the principle of protein-dye binding. Anal Biochem. 1976;72: 248–54.

125. Götze M, Pettelkau J, Schaks S, Bosse K, Ihling CH, Krauth F, et al. StavroX-A software for analyzing crosslinked products in protein interaction studies. J Am Soc Mass Spectrom. 2012;23: 76–87. doi:10.1007/s13361-011-0261-2

126. Andley UP. Crystallins in the eye: Function and pathology. Prog Retin Eye Res. 2007;26: 78–98. doi:10.1016/j.preteyeres.2006.10.003

127. Urban CF, Ermert D, Schmid M, Abu-Abed U, Goosmann C, Nacken W, et al. Neutrophil extracellular traps contain calprotectin, a cytosolic protein complex involved in host defense against Candida albicans. PLoS Pathog. 2009;5. doi:10.1371/journal.ppat.1000639

128. Thomas EL, Grisham MB, Jefferson MM. Myeloperoxidase-dependent effect of amines on functions of isolated neutrophils. J Clin Invest. 1983;72: 441–54.

129. Ronsein GE, Winterbourn CC, Di Mascio P, Kettle AJ. Cross-linking methionine and amine residues with reactive halogen species. Free Radic Biol Med. 2014;70: 278–287. doi:10.1016/j.freeradbiomed.2014.01.023

130. Asaria RH, Kon CH, Bunce C, Charteris DG, Wong D, Luthert PJ, et al. How to predict proliferative vitreoretinopathy: a prospective study. Ophthalmology. 2001;108: 1184–6.

131. Pastor JC, Rojas J, Pastor-Idoate S, Lauro S Di, Gonzalez-Buendia L, Delgado-Tirado S. Proliferative vitreoretinopathy: A new concept of disease pathogenesis and practical consequences. Prog Retin Eye Res. 2016;51: 125–155. doi:10.1016/j.preteyeres.2015.07.005

132. Pastor JC, Rodríguez E, Marcos MA, Lopez MI. Combined pharmacologic therapy in a rabbit model of proliferative vitreoretinopathy (PVR). Ophthalmic Res. Karger Publishers; 2000;32: 25–9. doi:10.1159/000055583

133. Asaria RH, Kon CH, Bunce C, Charteris DG, Wong D, Khaw PT, et al. Adjuvant 5-fluorouracil and heparin prevents proliferative vitreoretinopathy : Results from a randomized, double-blind, controlled clinical trial. Ophthalmology. 2001;108: 1179–83.

134. Vázquez-Chona F, Song BK, Geisert EE. Temporal changes in gene expression after injury in the rat retina. Invest Ophthalmol Vis Sci. 2004;45: 2737–46. doi:10.1167/iovs.03-1047

135. Alge CS, Priglinger SG, Neubauer AS, Kampik A, Zillig M, Bloemendal H, et al. Retinal pigment epithelium is protected against apoptosis by alphaB-crystallin. Invest Ophthalmol Vis Sci. 2002;43: 3575–82.

136. Bhat SP, Gangalum RK. Secretion of αB-Crystallin via exosomes: New clues to the function of human retinal pigment epithelium. Commun Integr Biol. 2011;4: 739–41.

137. Hong SM, Yang YS. A potential role of crystallin in the vitreous bodies of rats after ischemia-reperfusion injury. Korean J Ophthalmol. 2012;26: 248–54. doi:10.3341/kjo.2012.26.4.248

138. Yan H, Peng Y, Huang W, Gong L, Li L. The Protective Effects of αB-Crystallin on Ischemia-Reperfusion Injury in the Rat Retina. J Ophthalmol. 2017;2017: 7205408. doi:10.1155/2017/7205408

139. Aretz S, Krohne TU, Kammerer K, Warnken U, Hotz-Wagenblatt A, Bergmann M, et al. In-depth mass spectrometric mapping of the human vitreous proteome. Proteome Sci. 2013;11: 22. doi:10.1186/1477-5956-11-22

140. Zhou Q, Xu G, Zhang X, Cao C, Zhou Z. Proteomics of post-traumatic proliferative vitreoretinopathy in rabbit retina reveals alterations to a variety of functional proteins. Curr Eye Res. 2012;37: 318–26. doi:10.3109/02713683.2011.635397

141. Wang H, Feng L, Hu J, Xie C, Wang F. Differentiating vitreous proteomes in

proliferative diabetic retinopathy using high-performance liquid chromatography coupled to tandem mass spectrometry. Exp Eye Res. 2013;108: 110–119. doi:10.1016/j.exer.2012.11.023

142. Hall B, Limaye A, Kulkarni AB. Overview: generation of gene knockout mice. Curr Protoc cell Biol. 2009;Chapter 19: Unit 19.12 19.12.1–17. doi:10.1002/0471143030.cb1912s44

143. Priglinger SG, Alge CS, Kook D, Thiel M, Schumann R, Eibl K, et al. Potential role of tissue transglutaminase in glaucoma filtering surgery. Invest Ophthalmol Vis Sci. 2006;47: 3835–45. doi:10.1167/iovs.05-0960

144. Sohn J, Kim T-I, Yoon Y-H, Kim J-Y, Kim S-Y. Novel transglutaminase inhibitors reverse the inflammation of allergic conjunctivitis. J Clin Invest. 2003;111: 121–8. doi:10.1172/JCI15937

145. Lee S-M, Jeong EM, Jeong J, Shin D-M, Lee H-J, Kim H-J, et al. Cysteamine Prevents the Development of Lens Opacity in a Rat Model of Selenite-Induced Cataract. Investig Opthalmology Vis Sci. The Association for Research in Vision and Ophthalmology; 2012;53: 1452. doi:10.1167/iovs.11-8636

146. Groenen PJ, Bloemendal H, de Jong WW. The carboxy-terminal lysine of alpha B-crystallin is an amine-donor substrate for tissue transglutaminase. Eur J Biochem. 1992;205: 671–674.

147. Barathi VA, Weon SR, Tan QSW, Lin KJ, Tong L, Beuerman RW. Transglutaminases (TGs) in ocular and periocular tissues: Effect of muscarinic agents on TGs in scleral fibroblasts. PLoS One. 2011;6: 1–13. doi:10.1371/journal.pone.0018326

148. Fésüs L, Szondy Z. Transglutaminase 2 in the balance of cell death and survival. FEBS Lett. 2005;579: 3297–302. doi:10.1016/j.febslet.2005.03.063

149. Lentini A, Tabolacci C, Mattioli P, Provenzano B, Beninati S. Spermidine delays eye lens opacification in vitro by suppressing transglutaminase-catalyzed crystallin cross-linking. Protein J. 2011;30: 109–14. doi:10.1007/s10930-011-9311-7

150. Martinet N, Beninati S, Nigra TP, Folk JE. N1N8-bis(gamma-glutamyl)spermidine cross-linking in epidermal-cell envelopes. Comparison of cross-link levels in normal and psoriatic cell envelopes. Biochem J. 1990;271: 305–8.

151. Balajthy Z, Csomós K, Vámosi G, Szántó A, Lanotte M, Fésüs L. Tissue-

transglutaminase contributes to neutrophil granulocyte differentiation and functions. Blood. 2006;108: 2045–54. doi:10.1182/blood-2004-02-007948

12. Supplement

Supplementary figure 1. Representative results illustrating the workflow of crosslink detection using StavroX software. *The sequence of possible lysine and glutamine donor (K donor and Q donor) protein in FASTA format is shown on panel A and B. All the possible crosslinks between the K and Q residues are mapped and the results are given in form of spectrum and series of b and y ions. The panel C shows a spectrum with positive result. Based on the data represented in the spectrum the crosslink formed between the peptides highlighted in blue and red, respectively is drawn (panel D). In this way we can get information on the exact position of the amino acid residues and the sequence of the crosslinked tryptic peptides.*

A. **>sp|P02788|20-710 Lactotransferrin**

GRRRSVQWCAVSQPEATKCFQWQRNMRKVRGPPVSCIKRDSPIQCIQAIAENRADAVTLDGGFIYEAGLAPYKLRPVAAEVYGTERQPRTHY
YAVAVVKKGGSFQLNELQGLKSCHTGLRRTAGWNVPIGTLRPFLNWTGPPEPIEAAVARFFSASCVPGADKGQFPNLCRLCAGTGENKCAFSS
QEPYFSYSGAFKCLRDGAGDVAFIRESTVFEDLSDEAERDEYELLCPDNTRKPVDKFKDCHLARVPSHAVVARSVNGKEDAIWNLLRQAQEKF
GKDKSPKFQLFGSPSGQKDLLFKDSAIGFSRVPPRIDSGLYLGSGYFTAIQNLRKSEEEVAARRARVVWCAVGEQELRKCNQWSGLSEGSVTC
SSASTTEDCIALVLKGEADAMSLDGGYVYTAGKCGLVPVLAENYKSQQSSDPDPNCVDRPVEGYLAVAVVRRSDTSLTWNSVKGKKSCHTA
VDRTAGWNIPMGLLFNQTGSCKFDEYFSQSCAPGSDPRSNLCALCIGDEQGENKCVPNSNERYYGYTGAFRCLAENAGDVAFVKDVTVLQNT
DGNNNEAWAKDLKLADFALLCLDGKRKPVTEARSCHLAMAPNHAVVSRMDKVERLKQVLLHQQAKFGRNGSDCPDKFCLFQSETKNLLFN
DNTECLARLHGKTTYEKYLGPQYVAGITNLKKCSTSPLLEACEFLRK

B. **>sp|P05164|165-745 Myeloperoxidase**

MGVPFFSSLRCMVDLGPCWAGGLTAEMKLLLALAGLLAILATPQPSEGAAPAVLGEVDTSLVLSSMEEAKQLVDKAYKERRESIKQRLRSG
SASPMELLSYFKQPVAATRTAVRAADYLHVALDLLERKLRSLWRRPFNVTDVLTPAQLNVLSKSSGCAYQDVGVTCPEQDKYRTITGMCN
NRRSPTLGASNRAFVRWLPAEYEDGFSLPYGWTPGVKRNGFPVALARAVSNEIVRFPTDQLTPDQERSLMFMQWGQLLDHDLDFTPEPAAR
ASFVTGVNCETSCVQQPPCFPLKIPPNDPRIKNQADCIPFFRSCPACPGSNITIRNQINALTSFVDASMVYGSEEPLARNLRNMSNQLGLLAVN
QRFQDNGRALLPFDNLHDDPCLLTNRSARIPCFLAGDTRSSEMPELTSMHTLLLREHNRLATELKSLNPRWDGERLYQEARKIVGAMVQIIT
YRDYLPLVLGPTAMRKYLPTYRSYNDSVDPRIANVFTNAFRYGHTLIQPFMFRLDNRYQPMEPNPRVPLSRVFFASWRVVLEGGIDPILRGL
MATPAKLNRQNQIAVDEIRERLFEQVMRIGLDLPALNMQRSRDHGLPGYNAWRRFCGLPQPETVGQLGTVLRNLKLARKLMEQYGTPNNI
DIWMGGVSEPLKRKGRVGPLLACIIGTQFRKLRDGDRFWWENEGVFSMQQRQALAQISLPRIICDNTGITTVSKNNIFMSNSYPRDFVNCSTL
PALNLASWREAS

C.

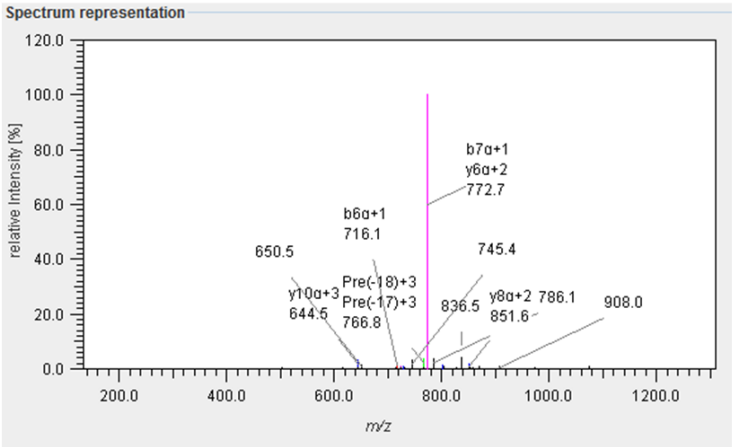

D.

Supplementary table 1. Representative results of the detected crosslinks between NET proteins obtained from donor 2 upon different treatments. *The type and position of crosslink, the name of proteins and the tryptic sequences participating in the crosslink are indicated. The one letter code is used for the amino acids.*

Ctrl					
Cross-link type	**Cross-link position**	**K donor protein**	**Q donor protein**	**K donor sequence**	**Q donor sequence**
ε-(γ-glutamyl)-lysine	K556-Q575	MPO	MPO	GLMATPAK (549-556)	LFEQVMR (572-578)
	K155/158-Q517	CTSG	MPO	LKTGK (154-158)	LDNRYQPMEPNPR (512-524)
	K212-Q589	CTSG	MPO	AMDQK (208-212)	IGLDLPALNMQRSR (579-592)
	K592-Q71	CTSG	MPO	EYWLVK (292-297)	QLVDK (71-75)
Cross-link type	**Cross-link position**	**K1 donor protein**	**K2 donor protein**	**K1 donor sequence**	**K2 donor sequence**
Bis-ε-lysyl SPM	K33-K108	CTSG	CTSG	KTYGK (33-37)	VPSQWQRNITYK (97-108)
Bis-ε-lysyl SPD	K18-K32	HIST1H2B	AZU1	KGFKK (14-18)	KARPR (32-36)
Bis-ε-lysyl PUT	K50-K29/30	S100A9	HIST1H2B	DLQNFLK (44-50)	EGKKRKR (27-33)
	K54-K50	CTSG	S100A9	RLIWEK (49-54)	DLQNFLK (44-50)
	K21-K108	HIST1H4	CTSG	KVLR (21-24)	NITYKSNPNR (104-113)
	K93-K92	S100A9	HIST1H4	LTWASHEK (86-93)	TVTAMDVVYALKR (81-93)
	K93-K45/48	S100A9	HIST1H2B	LTWASHEK (86-93)	ESYSIYIYKVLK (37-48)
Cross-link type	**Cross-link position**	**Q1 donor protein**	**Q2 donor protein**	**Q1 donor sequence**	**Q2 donor sequence**
Bis-γ-glutamyl SPM	Q18/Q22-Q455	CAT	CAT	EQRAAQK	AFYVNVLNEEQRKR
	Q306-Q195	MPO	CAT	IKNQADBIPFFR	PESLHQVSFLFSDR
Bis-γ-glutamyl SPD	Q18/22-Q455	CAT	CAT	EQRAAQK (17-23)	AFYVNVLNEEQRKR (445-458)
	Q306-Q195	MPO	CAT	IKNQADBIPFFR (303-314)	PESLHQVSFLFSDR (190-203)
$BPNH_2$ treatment					
Cross-link type	**Cross-link position**	**K donor protein**	**Q donor protein**	**K donor sequence**	**Q donor sequence**
ε-(γ-glutamyl)-lysine	K22/25-Q589	HIST1H2B	MPO	AVVKTQK (19-25)	LFEQVMRIGLDLPALNMQR (572-590)
	K625-Q46	MPO	S100A9	NLKLAR (623-628)	KDLQNFLKK (43-51)
	K13-Q589	HIST1H2B	MPO	GATISK (8-13)	IGLDLPALNMQRSR (579-592)
	K192-Q141/144	HIST1H4	LYZ	LLRK (189-192)	QYVQGBGV (141-149)
	K327-Q635/636	TLK	LTF	KAYGQALAK (319-327)	QVLLHQQAK (630-638)
Cross-link type	**Cross-link position**	**K1 donor protein**	**K2 donor protein**	**K1 donor sequence**	**K2 donor sequence**
Bis-ε-lysyl SPM	K260-K296/299	LTF	LTF	PVDKFK (257-262)	QAQEKFGK (292-299)
	K13/17-K50/51	HIST1H4	S100A9	GLGKGGAK (10-17)	ELVRKDLQNFLKK (39-51)
Bis-ε-lysyl SPD	K473-K376	LTF	LTF	SDTSLTWNSVK (463-473)	VVWBAVGEQELRK (364-376)
	K6-K96	HIST1H4	HIST1H2A	GKGGKGLGK (5-13)	NDEELNK (90-96)
	K6/9-K17	HIST1H4	HIST1H4	GKGGK (5-9)	GGAKR (14-18)
Bis-ε-lysyl PUT	K649-K473/475	LTF	LTF	FGRNGSDBPDK (639-649)	RSDTSLTWNSVKGK (462-475)
	K233/239-K103/105	ENO1	ENO1	TAIGKAGYTDK (229-239)	IDKLMIEMDGTENKSK (90-105)
	K37-K20	CTSG	CTSG	KTYGKQYK (33-40)	RLVBVLLVBSSAVAQLHK (3-20)
	K128-K17	HIST1H2B	HIST1H4	YTSSK (123-128)	GLGKGGAKRHR (10-20)
	K37-K78	HIST1H2A	MPO	LLRK (34-37)	QLVDKAYKER (71-80)
Cross-link type	**Cross-link position**	**M donor protein**	**K donor protein**	**M donor sequence**	**K donor sequence**
ε-lysyl-S-methionyl PUT	M577-K13/14	MPO	HIST1H2B	LFEQVMRIGLDLPALNMQR (572-590)	GATISKK (8-14)
Cross-link type	**Cross-link position**	**Q1 donor protein**	**Q2 donor protein**	**Q1 donor sequence**	**Q2 donor sequence**
Bis-γ-glutamyl PUT	Q399-Q269/272/277/279	TLK	TLK	AFDQIR (396-401)	NMAEQIIQEIYSQIQSKKK (265-283)

SPM treatment					
Cross-link type	**Cross-link position**	**K donor protein**	**Q donor protein**	**K donor sequence**	**Q donor sequence**
ε-(γ-glutamyl)-lysine	K103-Q359/367	MPO	MPO	SGSASPMELLSYFK (90-103)	NMSNQLGLLAVNQR (355-368)
	K16-Q455	CAT	MPO	DPASDQMQHWKEQR (6-19)	KIVGAMVQIITYR (448-460)
	K477/480-Q257	CAT	MPO	KAVK (477-480)	SLMFMQWGQLLDHDLDFTPEPAAR (249-272)
	K671-Q689/690	MPO	MPO	KLRDGDR (617-677)	DGDRFWWENEGVFSMQQR (674-691)
	K423-Q455	LTF	MPO	GEADAMSLDGGYVYTAGK (406-423)	KIVGAMVQIITYR (448-460)
	K649-Q314	LTF	LTF	FGRNGSDBPDK (639-649)	FGKDKSPKFQLFGSPSQK (297-315)
	K85-Q506	MPO	MPO	RESIK (81-85)	IANVFTNAFRYGHTLIQPFMFR (490-511)
	K17-Q86	HIST1H4	MPO	GLGKGGAK (10-17)	RESIKQR (81-87)
	K25-Q689/690	HIST1H2B	MPO	GFKKAVVKTQK (15-25)	DGDRFWWENEGVFSMQQR (674-691)
	K38-Q575	HIST1H3	MPO	KPHR (38-41)	LFEQVMR (572-578)
	K54-Q7	CTSG	HIST1H2A	RLIWEK (49-54)	GKQGGK (5-10)
	K123-Q104	HIST1H3	MPO	VTIMPKDIQLARR (118-130)	QPVAATR (104-110)
	K26/30-Q77	HIST1H2B	HIST1H3	KEGKK (26-30)	EIAQDFK (74-80)
	K35/36-Q100/102	S100A8	CTSG	DDLKK (32-36)	VPSQWQRNIITYKSNPNR (97-113)
Cross-link type	**Cross-link position**	**K1 donor protein**	**K2 donor protein**	**K1 donor sequence**	**K2 donor sequence**
Bis-ε-lysyl SPM	K10/14/16-K93	HIST1H2A	S100A9	QGGKVRAKAKSR (7-18)	QLSFEEFIMLMARLTWASHEK (73-93)
	K10/14/16-K25	HIST1H2A	S100A9	QGGKVRAKAKSR (7-18)	MSQLERNIETIINTFHQYSVK (5-25)
	K33-K108	CTSG	CTSG	KTYGK (33-37)	VPSQWQRNITYK (97-108)
Bis-ε-lysyl SPD	K629-K28	LTF	MPO	MDKVERLK (622-629)	BMVDLGPBWAGGLTAEMK (11-28)
	K624-K239	LTF	MPO	MDKVER (622-627)	AGYTDKVVIGMDVAASEFFR (234-253)
	K625-K37	MPO	LTF	NLKLAR (623-627)	SVQWBAVSQPAETKBFQWQR (24-43)
	K654-K448	MPO	MPO	KGRVGPLLABIIGTQFR (654-670)	LYQEARKIVGAMVQIITYR (442-460)
	K31-K25/26	LYZ	HIST1H2B	TLKR (29-32)	AVVKTQKKEGK (19-29)
	K14-K304	HIST1H2A	MPO	AKAK (13-16)	IPPNDPRIK (296-304)
	K19/24-K42	HIST1H3	CTSG	KQLATK (19-24)	EKNEEAVR (41-48)
	K212-K37	CTSG	HIST1H2A	AMDQK (208-212)	LLRKGNYEAR (34-43)
	K14-K31	HIST1H2A	LYZ	AKAK (13-16)	TLKR (29-32)
	K10-K84	HIST1H3	S100A8	KSTGGK (10-15)	MGVAAHK (78-84)
Bis-ε-lysyl PUT	K47-K649	LTF	LTF	NMRK (44-47)	FGRNGSDBPDKFBLFQSETK (639-658)
	K75-K129	MPO	MPO	QLVDKAYK (71-78)	AADYLHVALDLLERKLR (115-131)
	K85-K233	MPO	CAT	ESIK (82-85)	HMNGYGSHTFKLVNANGEAVYBK (211-233)
	K5-K233/239	ENO1	ENO1	MSILK (0-5)	TAIGKAGYTDKVVIGMDVAASEFFR (229-253)
	K556-K103/105	MPO	ENO1	GLMATPAK (549-556)	IDKLMIEMDGTENKSK (90-105)
	K45-K304	HIST1H4	MPO	RGGVKR (41-46)	IPPNDPRIK (296-304)
	K625/629-K7	MPO	S100A8	NLKLARK (623-629)	MLTELEK (0-7)
	K5-K24	HIST1H3	HIST1H3	MARTK (0-5)	KQLATK (19-24)
	K10-K37	HIST1H2A	HIST1H2A	QGGKAR (7-12)	LLRKGNYAER (34-43)
	K9-K40	HIST1H4	CTSG	GGKGLGKGGAKR (7-18)	TYGKQYKEK (34-42)

Cross-link type	Cross-link position	M donor protein	K donor protein	M donor sequence	K donor sequence
ε-lysyl-S-methionyl SPM	M81-K10/14/16	S100-A9	H2A	QLSFEEFIMLMARLTWASHEK (73-93)	QGGKVRAKAKSR (7-18)
	M5-K123	S100-A9	H3	RVTIMPK (117-123)	MSQLER (5-10)
ε-lysyl-S-methionyl SPD	M575-K281	MPO	TLK	LFEQVMR (572-578)	NMAEQIIQEIYSQIQSK (265-281)
	M5-K14/16	S100A9	HIST1H2A	MSQLER (5-10)	ARAKAKTR (11-18)
	M0-K629	S100A9	MPO	MTBK (0-4)	LARK (626-629)
ε-lysyl-S-methionyl PUT	M212-K457	CAT	CAT	HMNGYGSHFK (211-221)	AFYVNVLNEEQRKR (445-458)
	M244-K5	ENO1	ENO1	MSILK (0-5)	VVIGMDVAASEFFRSGKYDLDFK (240-262)
	M97-K556	ENO1	MPO	IDKLMIEMDGTENKSK (90-105)	GLMATPAK (549-556)
Cross-link type	**Cross-link position**	**Q1 donor protein**	**Q2 donor protein**	**Q1 donor sequence**	**Q2 donor sequence**
Bis-γ-glutamyl SPM	Q444-Q200	MPO	ELANE	LYQEARK (442-448)	MMYQKKKFAYGYIEDLK (197-213)
	Q20-Q97	H3	H2B	APRKQLATKAAR (16-27)	EIQTAVRLLLPGELAK (95-110)
	Q560/562-Q161	MPO	MPO	QNQIAVDEIR (560-569)	SSGBAYQDVGVTBPEQDK (155-172)
Bis-γ-glutamyl SPD	Q292/294-Q575/589	LTF	MPO	EDAIWNLLRQAQEK (283-296)	LFEQVMRIGLDLPALNMQR (572-590)
	Q306/314-Q506	LTF	MPO	SPKFQLFGSPSGQK (302-315)	YGHTLIQPFMFR (500-511)
	Q126-Q124	HIST1H3	HIST1H2A	DIQLAR (124-129)	KTESQKTK (120-127)
Bis-γ-glutamyl PUT	Q444-Q654	MPO	LTF	LYQEAR (442-447)	FGRNGSDBPDKFBLFQSETK (639-658)
	Q24-Q46	HIST1H2B	S100A9	TQKK (23-26)	KDLQNFLK (43-50)
	Q370-Q24	MPO	HIST1H2B	FQDNGR (369-374)	AVVKTQK (19-25)